Field Ionization and Field Desorption

8

Learning Objectives

- Ion formation by action of very strong electric fields
- Desorption of ions into the gas phase by strong electric fields
- Softness of field ionization and field desorption
- Methods of sample introduction for field ionization and field desorption
- General properties and fields of application of the title methods
- Applications to air- and moisture-sensitive samples
- Complex mixture analysis by combining gas chromatography and high-resolution mass spectrometry with field ionization and field desorption

8.1 Evolution of Field Ionization and Field Desorption

The first observation of the desorption of positive ions from surfaces by high electrostatic fields was made by means of a field ion microscope [1, 2]. The mass spectrometric analysis of some field-ionized gases followed soon [2–4]. In 1959, H. D. Beckey presented the first focusing field ionization ion source [5]. In these early experiments electric field strengths of about 10^8 V cm^{-1} (1 V$Å^{-1}$) were generated at sharp tungsten tips [2, 4, 5]. The method of *field ionization* (FI) was soon extended to analyzing volatile liquids [6–10] and solids introduced by evaporation from a sample vial in close proximity to the ionizing tip or wire electrode [11]. FI, still embryonic in the mid-1960s, had soon to compete with chemical ionization (CI, Chap. 7) [12]. The major breakthrough came from its further development to *field desorption* (FD), because FD circumvents the evaporation of the analyte prior to ionization [13, 14]. Instead, the processes of ionization *and* subsequent desorption of the formed ions are centered on the surface of the *field*

J.H. Gross, *Mass Spectrometry*, DOI 10.1007/978-3-319-54398-7_8

emitter. The specific charm of FI-MS and especially of FD-MS arises from their extraordinary softness of ionization, in many cases yielding solely intact molecular ions, and from the capability of FD to handle neutral as well as ionic analytes [15–24]. FD-MS initially flourished from the mid-1970s to the mid-1980s, but soon suffered from the advent of fast-atom bombardment (FAB) and later electrospray ionization (ESI) mass spectrometry [23]. Then, however, the unique capabilities of FD-MS were rediscovered [25–27], even more so with the advent of advanced sample introduction [28, 29] and the adaptation of FI and FD ion sources to oaTOF and FT-ICR mass analyzers [30–35].

8.2 Field Ionization Process

Inghram and Gomer described and explained the process of *field ionization* of a single hydrogen atom [3, 4, 36]: If a hydrogen atom resides on a metal surface, its proton-electron potential is only slightly distorted. However, in the presence of an electric field in the order of 2 $V Å^{-1}$ (1 Å = 10^{-10} m) with the metal at positive polarity, this distortion becomes remarkable (Fig. 8.1). As a result, the electron can become detached from the proton by tunneling into the bulk metal through a potential barrier that is only a few angstroms wide and some electronvolts high [19, 37]. Thereby, the hydrogen atom becomes ionized, and the resulting proton is immediately driven away by action of the electric field. Interestingly, the situation is quite similar for an isolated hydrogen atom. Here, the electric field causes analogous distortion of the potential, and with sufficient field strength, the atom is field ionized, too. This means that atoms or molecules can be ionized by the mere action of a strong electric field independent of whether they have been adsorbed to the anodic surface or whether they are moving freely through the space between the electrodes.

Field ionization essentially is a autoionization-type process, i.e., an internally supra-excited atom or molecular moiety loses an electron spontaneously without further interaction with an energy source [38]. Different from electron ionization, there is no excess energy transferred onto the incipient ion, and thus, dissociation of the ions is reduced to a minimum.

$$M \rightarrow M^{+\bullet} + e^{-} \tag{8.1}$$

Electric fields sufficient to effect field ionization are only obtained in close proximity to sharp tips, edges, or thin wires. The smaller the radius of the curvature of the anode, the further away (1–10 nm) the field sufficing to cause ionization (Fig. 8.1). The importance of sufficient electric field strength is reflected by the extreme decrease in half-life calculated for a hydrogen atom: it is in the order of 0.1 s at 0.5 $V Å^{-1}$, 0.1 ns at 1.0 $V Å^{-1}$, and 0.1 f. at 2.5 $V Å^{-1}$ [19].

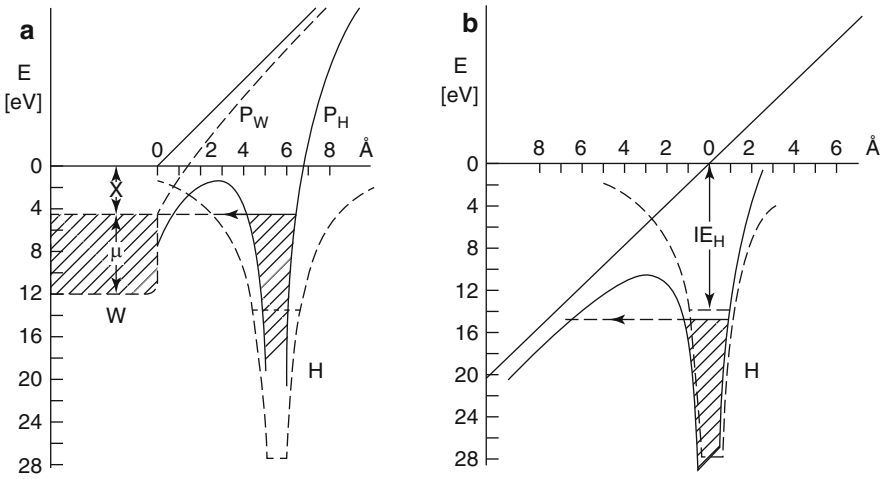

Fig. 8.1 Field ionization of a hydrogen atom (H) (**a**) close to a tungsten surface (*W*), (**b**) isolated. Conditions and symbols: electric field 2 VÅ^{-1}, P_W image potential of W distorted by the field, P_H potential of the hydrogen atom distorted by the field, X work function, μ Fermi level. *Dashed lines* represent potentials in absence of the electric field (Adapted from Ref. [4] by permission. © Verlag der Zeitschrift für Naturforschung, 1955)

Naming the parts

The field anode is usually referred to as *field emitter*, *FI emitter*, or *FD emitter*. The properties of the field emitter are of key importance for FI- and FD-MS. The electrode opposed to the emitter is called *field cathode* or simply *counter electrode*.

8.3 FI and FD Ion Sources

In FI- and FD-MS, a voltage of 8–12 kV is applied between *field emitter* (field anode) and *counter electrode* (field cathode) usually located 2–3 mm in front of the emitter. Thus, the desorbing ions are accelerated to 8–12 keV kinetic energy, clearly exceeding the amount which can be handled by a double-focusing magnetic sector instrument (typically used in conjunction with FI/FD ion sources). These contradictory requirements can be met by setting the counter electrode to negative potential to establish the high field gradient for ion generation while adjusting the difference between emitter and ground potential to the actual acceleration voltage (Fig. 8.2) [39]. With the emitter grounded and the counter electrode at high negative potential even slow ion beams can be delivered for mounting FD ion sources to FT-ICR or oaTOF instruments [30, 40].

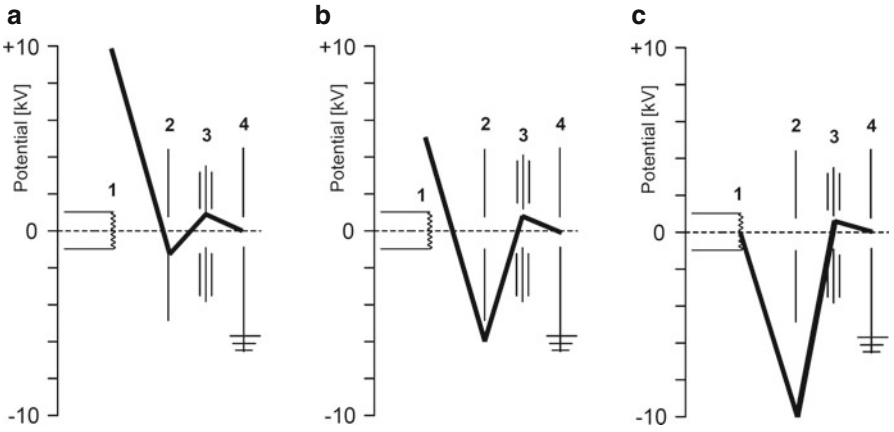

Fig. 8.2 Potentials (*bold lines*) along different FI/FD ion sources to realize full extraction voltage while delivering ions of defined kinetic energy to the analyzer. The part numbers correspond to: (*1*) emitter, (*2*) counter electrode, (*3*) optional electrostatic lenses, (*4*) analyzer entrance slit. (**a**) Instruments with high acceleration voltage, (**b**) instruments with medium acceleration voltage as is often the case in magnetic sector instruments, and (**c**) instruments requiring slow ions, e.g., FT-ICR or oaTOF instruments

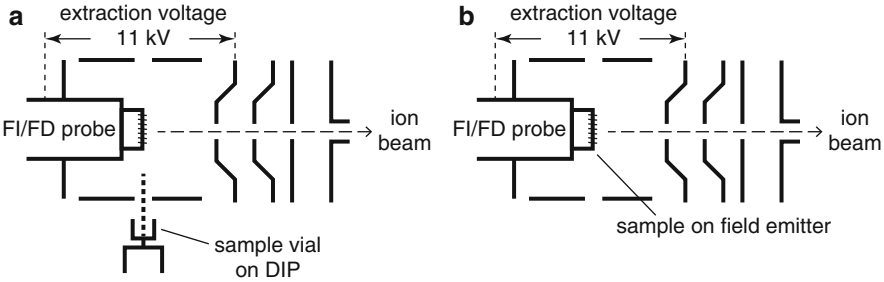

Fig. 8.3 Schematic of an FI/FD ion source (**a**) in FI mode, (**b**) in FD mode. The distance between emitter and counter electrode is exaggerated for clarity (Adapted from Ref. [41] by permission. © Springer-Verlag, Heidelberg, 1991)

In FI mode, the analyte is introduced via external inlet systems such as a direct probe, a reservoir inlet, or a gas chromatograph (Sects. 5.2 and 5.4). In FD mode, the analyte is supplied directly on the surface of the field emitter. Doing so not only guarantees a more efficient usage of the sample, it also combines the steps of ionization and desorption, thereby minimizing the risk of thermal decomposition prior to ionization (Figs. 8.3 and 8.4). This is especially important in case of highly polar or ionic analytes that cannot be evaporated without thermal degradation.

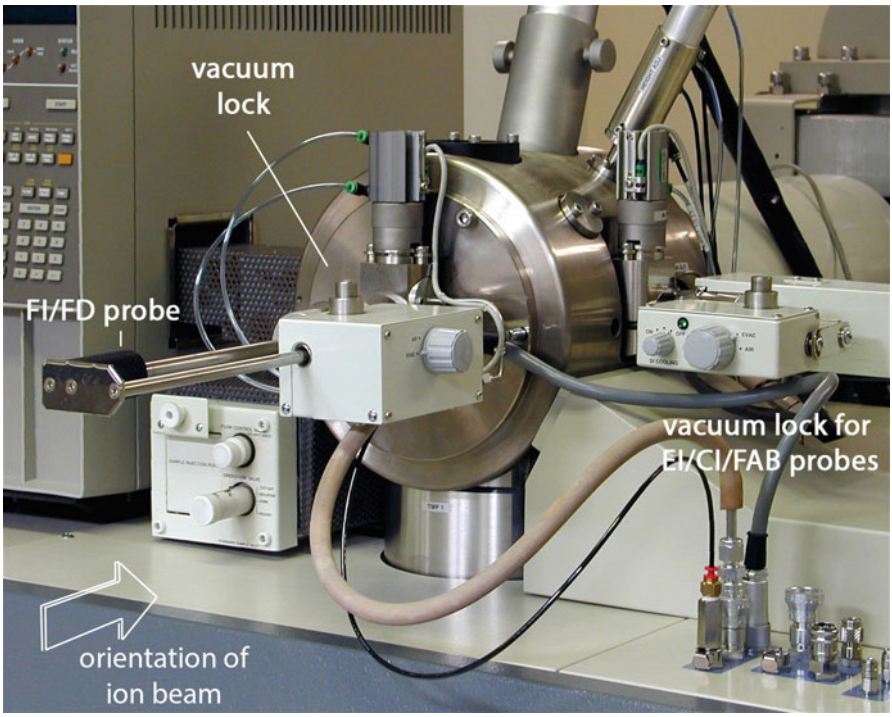

Fig. 8.4 FD probe inserted into the vacuum lock. FD probes are generally inserted in axial position to free the vacuum lock of the DIP for FI use. The emitter wire is now oriented vertically to comply with the beam geometry of the magnetic sector analyzer

8.4 Field Emitters

8.4.1 Blank Metal Wires as Emitters

In the first FI experiments, the high electric field strength was obtained at sharply pointed tungsten tips [2, 4, 5]. Later, edges of sharp blades [42] and wires of a few micrometers in diameter were used. Wires are advantageous because the emitting surface of a smooth blade is approximately two orders of magnitude smaller than that of a smooth wire at the same field strength under normal working conditions (Fig. 8.5). Simple wire emitters can be used for field desorption of nonpolar [43] or electrolytic analytes [44]. As thin wires are fragile and can break during electric discharges, sharp edges should be avoided in their vicinity, e.g., by polishing the counter electrode [45].

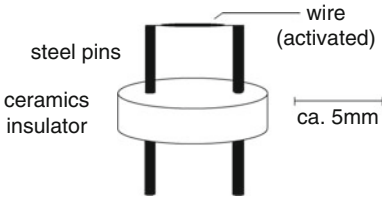

Fig. 8.5 A wire emitter: high voltage is supplied via the emitter-holding pins. These also serve to pass a current for resistive heating through the (activated) wire

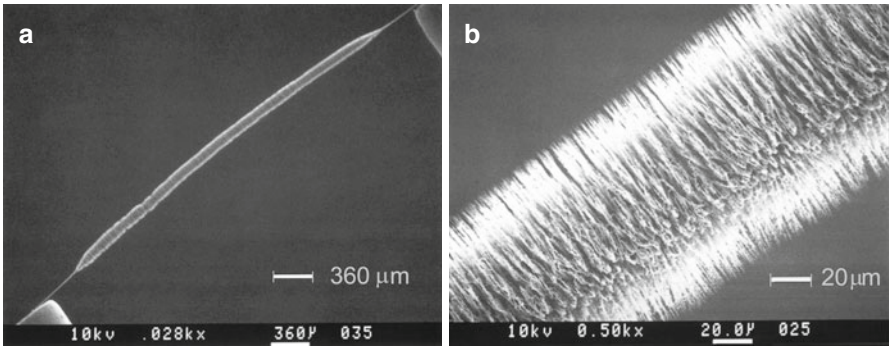

Fig. 8.6 SEM pictures of activated tungsten wire emitters; (**a**) overview showing the thin tungsten wire close to the holders and the whisker-bearing middle section, (**b**) detail of the central part revealing whiskers (By courtesy of Carbotec, Bergisch Gladbach, Germany)

8.4.2 Activated Emitters

The electric field strength on the emitter can greatly be enhanced by creating dendritic microneedles (*whiskers*) on its surface, by a process known as *emitter activation*. FI- and FD-MS require emitters of reproducible high quality, and therefore the activation procedure has received much attention. The high-temperature activation of 10 µm tungsten wires with pure benzonitrile vapor takes 3–7 h [46], but it may be accelerated by reversal of the polarity of the high voltage during activation [47], or by using indane, indene, indole, or naphthalene as the activating agent [48]. The activation procedures with benzonitrile or indene are employed commercially to produce carbon whiskers on emitters (Fig. 8.6). Microneedle growth is also achieved by decomposition of hexacarbonyltungsten, $W(CO)_6$, on a cathode producing an electric discharge [49]. A self-controlling mechanism which draws ions preferably to the top of the growing tungsten needles has been suggested [49]. SEM pictures of activated emitter surfaces and single whiskers have an aesthetic appeal [47–52].

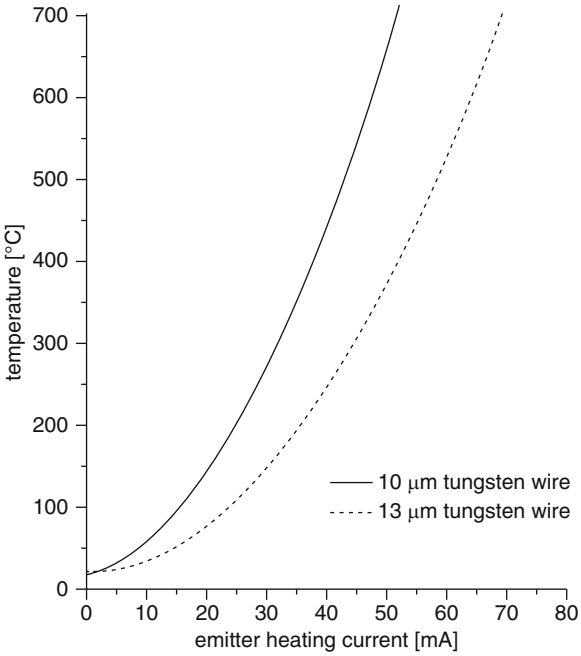

Fig. 8.7 Calibration of EHC vs. temperature for emitters activated with carbon needles on 10-μm and 13-μm tungsten wire (By courtesy of Carbotec, Bergisch Gladbach, Germany)

8.4.3 Emitter Temperature

Emitters can be heated by applying an electric current via the emitter holders. It is somewhat difficult to establish a precise calibration of emitter temperature versus *emitter heating current* (EHC) [53, 54]. The actual temperature not only depends on the emitter material, but also on diameter and length of the emitter as well as on length and area density of the whiskers. A useful estimate for tungsten emitters with carbon whiskers is given below (Fig. 8.7).

In practice, moderate heating of the emitter at constant current serves to reduce adsorption to its surface during FI measurements. Heating at a constant rate (1–20 mA min^{-1}) is frequently employed to enforce desorption of analytes from the emitter in FD-MS. Electric discharges resulting from too massive ion desorption can be avoided by emission-controlled emitter heating [55–57]. Where the EHC is regulated as to achieve a constant ion emission current, typically in the range of 1–100 nA. At the end, the emitter is cleaned for subsequent measurements by baking for 2–5 s at 800–1000 °C at 50–60 mA (activated tungsten emitters of 10 μm diameter) or at 80–100 mA (emitters of 13 μm).

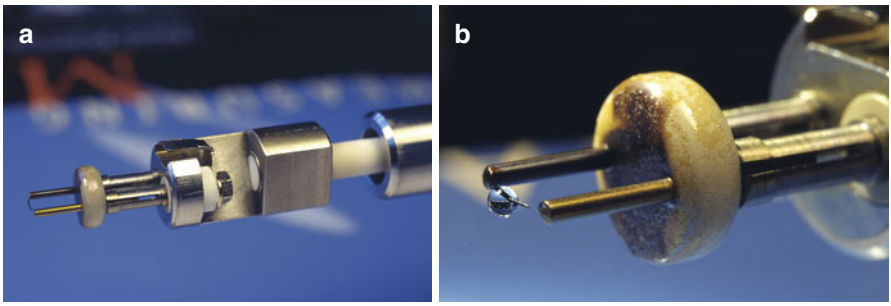

Fig. 8.8 FD probe. (**a**) Emitter holder of a JEOL FD probe tip, (**b**) a drop formed of 1–2 µl of analyte solution placed onto the activated emitter by means of a microliter syringe

8.4.4 Handling of Activated Emitters

Activated wire emitters are extremely fragile, because after activation the material behaves more like ceramics than like a metal wire. The slightest touch with a syringe needle as well as electric discharges during operation cause immediate destruction of the emissive wire. Delicate handling of the emitter is therefore a prerequisite [23]. Follow these guidelines for longer emitter lifespans:

- Use tweezers for emitter manipulation. Grasp the emitter either at the robust ceramics socket or at both steel pins simultaneously.
- Bake the emitter before first use in order to outgas and clean the emitter.
- When applying analyte solutions onto the emitter, only the emerging drop should come in contact with the emitter wire, but not the syringe needle (Fig. 8.8).
- Avoid excessive loading, as analyte solution may spread even onto the steel pins. From there, it can be washed back during loading of the subsequent sample.
- Allow complete evaporation of the solvent before insertion into the vacuum lock (Fig. 8.4).
- Switch on the high voltage only after the high vacuum has fully recovered.
- Switch off the high voltage after completion of the measurement.
- Finally, repeatedly bake the emitter to remove sample residues.

Adequate handling provided, an emitter can last for up to 20 measurements.

Better don't dip it

To apply a solution of the analyte, the emitter can either be *dipped into*, or alternatively, a drop of 1–2 µl can be *transferred onto* the emitter by means of a microliter syringe [52]. The latter method exhibits better reproducibility and avoids contamination of the emitter pins. Special micromanipulators are available to handle the syringe [14], but with some exercise a skilled operator can accomplish it manually.

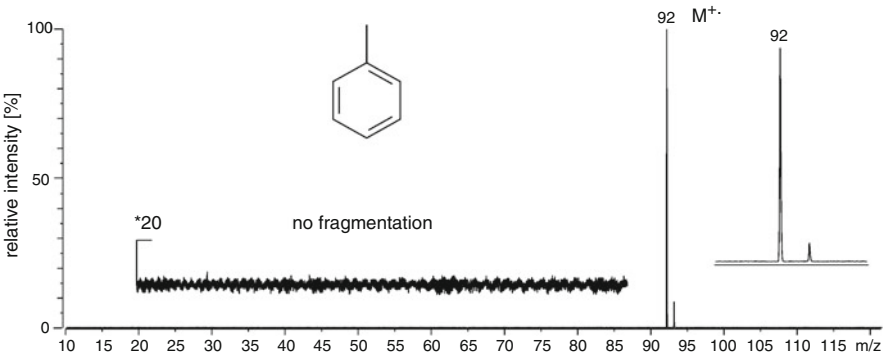

Fig. 8.9 FI spectrum of toluene. The molecular ion and its isotopolog are the only observed entities. (The CID spectrum of field-ionized toluene is shown in Sect. 9.3, the EI spectrum is discussed in Sect. 6.4)

8.5 Field Ionization Mass Spectrometry

FI mass spectra are normally characterized by intense molecular ion peaks accompanied by no or in some cases just a few fragment ions [9, 11, 58]. Especially in case of nonpolar low-mass analytes, FI-MS can serve for molecular ion mass spectrometry (Fig. 8.9) [59]. This property made FI-MS a standard tool for hydrocarbon analysis in the petroleum industry [6, 7, 10, 12, 25, 59–61]. FI performs nicely for samples that can reasonably be evaporized, but it exhibits poor sensitivity for polyhalogenated compounds such as $CHCl_3$ or PFK. FI usually fails with highly polar or even ionic compounds due to thermal decomposition. Nonetheless, there is no rule without exceptions: FI can, for example, create low-abundant "molecular ions", more appropriately described as cation-radical pairs $[C+A]^{+\bullet}$, of ionic liquids [62].

Although convenient at first sight, the lack of fragment ion peaks in FI spectra also means a lack of structural information. If data beyond a mere estimate of the elemental composition based on the isotopic pattern are asked for, then tandem MS employing collision-induced dissociation (CID, Chap. 9) is the preferred standard of structure elucidation. Fortunately, the fragmentation pathways of $M^{+\bullet}$ ions in CID are the same as in EI-MS (Chap. 6).

Low ion currents by FI

In FI-MS, the ionization efficiency is very low, because of the low probability for a neutral effusing from any inlet system towards the field emitter to come close enough to the whiskers. Consequently, FI-MS produces very low ion currents. The application of FI-MS is therefore restricted to samples that are too volatile for FD-MS or require prior gas chromatographic separation.

Table 8.1 Ions formed by FI

Analytes	Ions formed
Nonpolar	$M^{+\bullet}$, M^{2+}, occasionally $M^{3+\bullet}$, rarely $[M+H]^+$
Medium polarity	$M^{+\bullet}$, M^{2+} and/or $[M+H]^+$
Polar	$[M+H]^+$
Ionic	Generally thermal decomposition

8.5.1 Origin of $[M+H]^+$ Ions in FI-MS

FI mass spectra can show signals due to reactions of the analyte with the emitter surface or between molecules adsorbed to that surface. In case of acetone, it was demonstrated that $[M+H]^+$ ions are produced mainly by a *field-induced proton-transfer* reaction in the physically adsorbed layer [63]. The mechanism of this field-induced reaction depends on the existence of tautomeric structures of the neutral molecule. Besides the $[M+H]^+$ ions, $[M–H]^\bullet$ radicals are formed in an overall reaction analogous to CH_5^+ formation in CI:

$$M^{+\bullet} + M \rightarrow [M+H]^+ + [M-H]^\bullet \tag{8.2}$$

Furthermore, the radicals formed upon field-induced hydrogen abstraction can lead to polymerization products on the emitter surface [63]. Criteria to distinguish $M^{+\bullet}$ from $[M+H]^+$ ions have been published [64]. Besides analyte polarity and acidity of the solvent used for sample deposition onto the emitter, lower electric field strength and lower emitter temperature are likely to cause stronger $[M+H]^+$ ion contributions [64]. Analytes possessing exchangeable hydrogens strongly tend to form $[M+H]^+$ ions in FI-MS. Occasionally, the protonated molecule occurs in favor of the molecular ion that even may be hardly present (cf. Table 8.1).

8.5.2 Multiply-Charged Ions in FI-MS

Multiply charged ions of minor abundance are frequently observed in FI and FD mass spectra. Their increased abundance as compared to EI spectra can be rationalized by either of the following two-step processes: (*i*) *Post-ionization* of gaseous $M^{+\bullet}$ ions can occur due to the probability for an $M^{+\bullet}$ ion to suffer a second or even third ionization while drifting away from the emitter surface [65, 66]. Especially ions generated in locations not in close vicinity of the counter electrode pass numerous whiskers on their first 10–100 μm of flight:

$$M \rightarrow M^{+\bullet} + e^- \tag{8.3}$$

$$M^{+\bullet} \rightarrow M^{2+} + e^- \tag{8.4}$$

(*ii*) Alternatively, a surface-bound ion, $M^{+\bullet}{}_{(surf)}$, is formed and ionized for a second time before leaving the surface [67–69]:

$$M \rightarrow M^{+\bullet}{}_{(surf)} + e^- \tag{8.5}$$

$$M^{+\bullet}{}_{(surf)} \rightarrow M^{2+} + e^- \tag{8.6}$$

The most commonly formed types of ions in FI are summarized in Table 8.1.

Multiple charges compress *m/z* scale
For recognizing multiply charged ions, it is important to keep in mind that the *m*/*z* scale is compressed by a factor equal to the number of charges *z* (Sects. 3.8 and 4.2).

8.5.3 Field-Induced Dissociation

In certain cases, the advantageous property of the strong electric field to effect soft ionization can be accompanied by *field-induced dissociation*, another type of field-induced reactions [58, 70, 71]. For example, the fragment ions in the FI spectra of low-mass aliphatic amines, ketones, and hydrocarbons are formed by field-induced dissociation [58, 63]. Field-induced dehydrogenation [72, 73] presents a severe problem to the FI and FD analysis of saturated hydrocarbon mixtures reaching beyond C_{40}, because signals from unsaturated compounds at low levels are superimposed by $[M–H_2]^{+\bullet}$ peaks [74–77]. A reduction of the emitter potential can reduce field-induced dehydrogenation to some degree.

8.5.4 Accurate Mass FI Spectra

Accurate mass complements FI with other valuable information. Unfortunately, FI delivers very low ion currents, which on scanning sector instruments make it difficult to achieve accurate mass measurements. This is because (*i*) high resolution requires narrow slits, and thus, goes along with low transmission, and (*ii*) internal reference masses have to be distributed over the entire range making interferences more likely. While HR-FI-MS on sector instruments is neither new nor impossible [78–81], it is generally outside routine operation [62]. The attachment of FI/FD ion sources to oaTOF instruments has made it quite a bit easier, because a single point of reference, a so-called *lock mass*, is normally sufficient [30, 31].

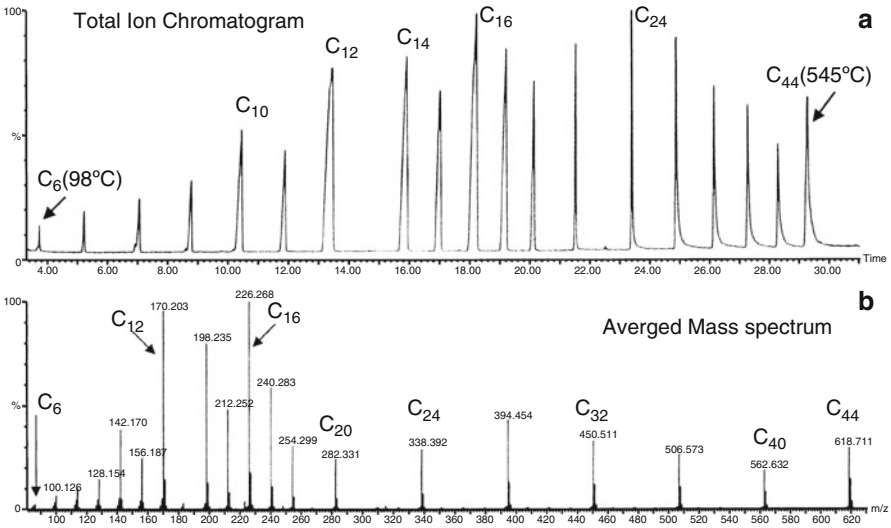

Fig. 8.10 GC-FI-oaTOF-MS total ion chromatogram and averaged mass spectrum of C_6–C_{44} *n*-paraffins. The masses of the paraffin molecular ions are all accurate (Reproduced from Ref. [31] with permission. © American Chemical Society, 2002)

8.5.5 Coupling Gas Chromatography to FI-MS

The coupling of gas chromatography to FI-MS was first attempted in the early 1970s [82, 83], but suffered from poor instrument capabilities of that time. Recent advances with oaTOF instrumentation allow for fast acquisition of spectra, comparatively high resolution, and more importantly, straightforward accurate mass measurements in GC-FI-MS. Thus, GC-FI-MS has become a trusted tool in several laboratories, especially in the petroleum community [30, 31, 84, 85]. To maintain full ionization efficiency, it is common that an accumulation period of 1 s per spectrum is followed by flash-heating the emitter for 0.1–0.2 s [30, 31]. These applications have also been driving the development of EI/FI/FD [40] and EI/CI/FI combination sources for GC-oaTOF instruments [86].

GC-FI-MS of paraffins GC-FI-oaTOF-MS measurements were performed on paraffins from C_6 to C_{44}, covering the wide boiling range from 98 to 545 °C, delivering GC separation and accurate mass information in one run. Main components such as the C_{12}, C_{14}, and C_{16} alkanes caused some broadening of their gas chromatographic peaks, eventually due to adsorption/desorption from the emitter surface resulting in a temporal spread [31]. Figure 8.10 shows the gas chromatogram as represented by the total ion chromatogram and the averaged mass spectrum over the complete acquisition period. Although FI of the entire mixture would have yielded a similar mass spectrum, this approach avoids mutual interference during ionization, and additionally, delivers isomer recognition from retention times.

8.6 FD Spectra

FD can be regarded the softest ionization method in mass spectrometry, even though electrospray ionization and matrix-assisted laser desorption ionization can transfer much larger ions into the gas phase [26, 87]. This is mainly because the ionization process itself does not transfer any extra energy to the incipient ions. Problems normally arise above molecular weights of 3000 u where the heated emitter causes thermal decomposition of the sample.

FD delivers $M^{+\bullet}$ of chlorotriphenylmethane The extraordinarily stable trityl ion, Ph_3C^+, *m*/*z* 243, tends to dominate mass spectra (Sect. 6.6.2). Thus, neither the EI spectrum of chlorotriphenylmethane nor that of its impurity triphenylmethanol show molecular ions (Fig. 8.11). An isobutane PICI spectrum also shows the trityl ion almost exclusively, although some hint is obtained from the Ph_2COH^+ ion, *m*/*z* 183, that cannot be explained as a fragment of a chlorotriphenylmethane ion. Only FD reveals the presence of the alcohol by its molecular ion at *m*/*z* 260, while that of the chloride is detected at *m*/*z* 278. Both molecular ions undergo some $OH^\bullet$ or $Cl^\bullet$ loss, respectively, to yield the Ph_3C^+ fragment ion of minor intensity.

8.6.1 Ion Formation by Field Ionization in FD-MS

In *field ionization* (as an experimental configuration) *field ionization* (the process) is the major pathway of ion generation. In *field desorption* from activated emitters, the analyte may also undergo *field ionization*. Presuming that the molecules are deposited in layers on the shanks of the whiskers or between them, this requires that (*i*) analytes of low polarity are polarized by action of the electric field, (*ii*) become mobile upon heating, and (*iii*) finally reach the locations of ionizing electric field strength at the tips of the whiskers (Fig. 8.12). The requirement of mobility of the polarized molecules can either be fulfilled via gas phase transport or surface diffusion [52]. As the level of mobility to travel some ten micrometers along a whisker is clearly below that for evaporation from a separate inlet system, thermal decomposition of the field-ionized analyte in FD-MS is much reduced as compared to FI-MS.

The relevance of the FI mechanism of ionization decreases as the polarity of the analyte increases. In certain cases such as sucrose, for example, it is not easy to decide whether gas phase mobility of the neutral and molecular ions jointly formed by FI still play a role [88, 89] or not [90].

EI, FI and FD mass spectra of D-Glucose D-Glucose evaporates into the ion source without complete decomposition as demonstrated by its FI spectrum (Fig. 8.13). FD yields a spectrum with a very low degree of fragmentation that is most probably due to the required slight heating of the emitter. The occurrence of $M^{+\bullet}$ ions, *m*/*z* 180, and $[M+H]^+$ ions, *m*/*z* 181, in the FD spectrum suggests that ion formation occurs via field ionization and field-induced proton transfer, respectively.

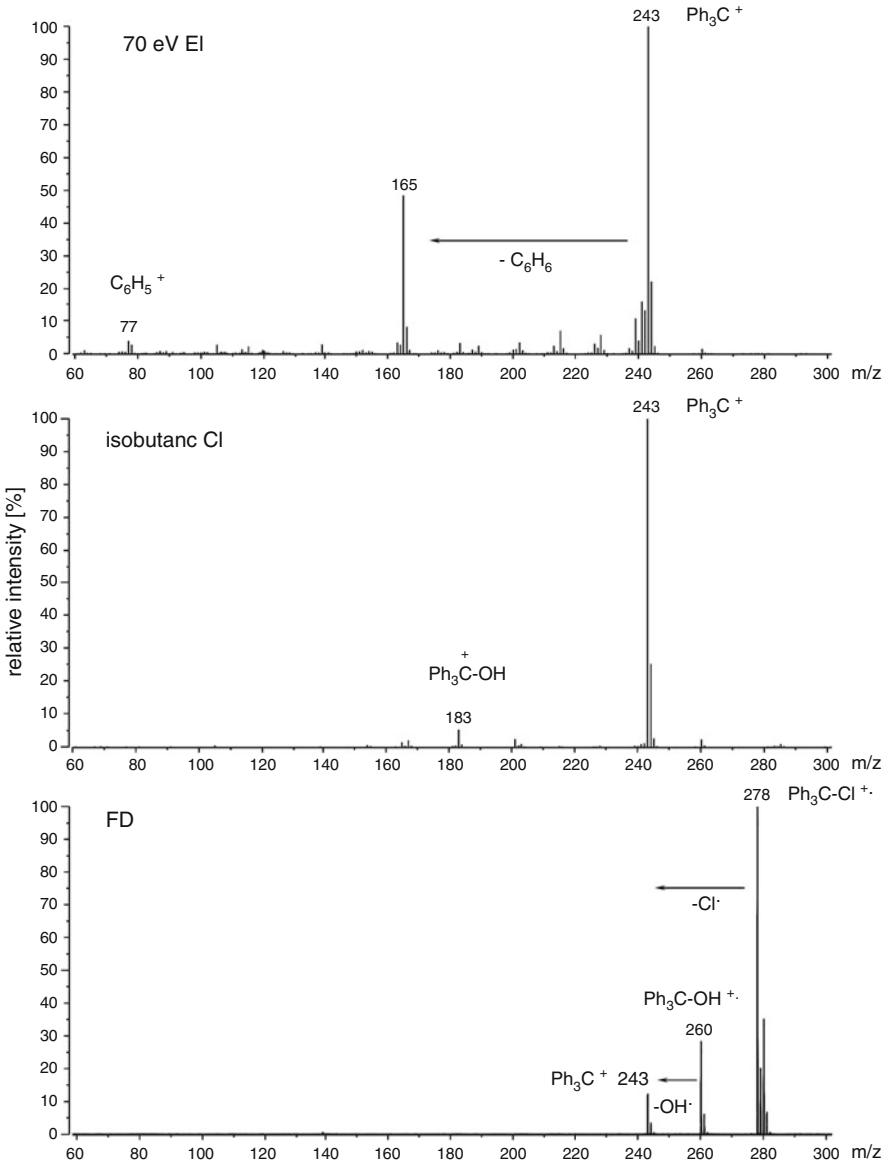

Fig. 8.11 Comparison of EI, PICI, and FD mass spectra of chlorotriphenylmethane containing some triphenylmethanol (By courtesy of C. Limberg, Humboldt University, Berlin)

However, thermal energy plus a hard ionization method (as EI) effect extreme fragmentation. By comparing the EI and FI spectra, the effects of thermal energy may roughly be distinguished from those of EI itself.

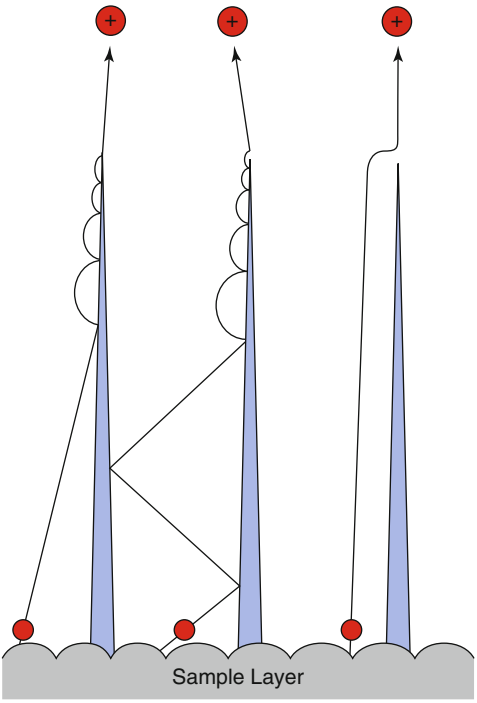

Fig. 8.12 The transport of neutrals to the tips of the field-enhancing whiskers (Reproduced from Ref. [52] by permission. © Elsevier Science, 1981)

8.6.2 Desorption of Preformed Ions in FD-MS

Analytes of very high polarity are not further ionized by field ionization. Here, the prevailing pathways are *protonation* or *cationization*, i.e., the attachment of alkali ions to molecules [91]. The subsequent desorption of the ions from the surface is effected by the action of the electric field. As $[M+Na]^+$ and $[M+K]^+$ ions are already present in the condensed phase, the field strength required for their desorption is lower than that for field ionization or field-induced $[M+H]^+$ ion formation [44, 92]. The desorption of ions is also effective in case of ionic analytes.

Bare wire emitters in FD-MS FD from untreated wire emitters to which alkali metal salts were added was used to obtain mass spectra of tartaric acid, arginine, pentobarbital, and other compounds [91, 93]. Besides $[M+H]^+$ ions, m/z 175, the FD mass spectrum of arginine exhibits $[M+Na]^+$, m/z 197, and $[M+K]^+$, m/z 213, ions due to alkali metal cationization as well as $[2M+H]^+$, m/z 349, cluster ions (Fig. 8.14) [44].

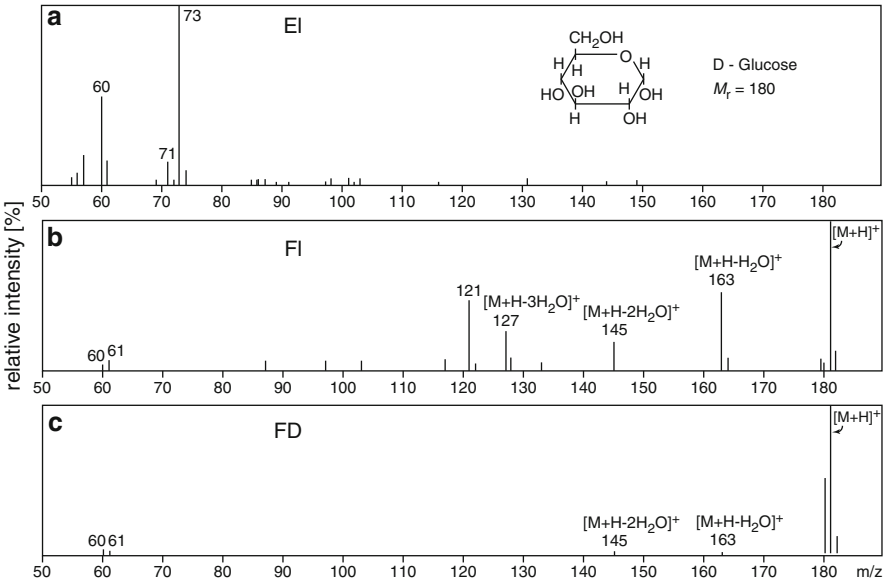

Fig. 8.13 D-Glucose mass spectra: (**a**) EI only yields ions that are due to decomposition and fragmentation, (**b**) FI still produces several fragments, and (**c**) FD almost exclusively gives ions related to the intact molecule (Adapted from Ref. [13] by permission. © Elsevier Science, 1969)

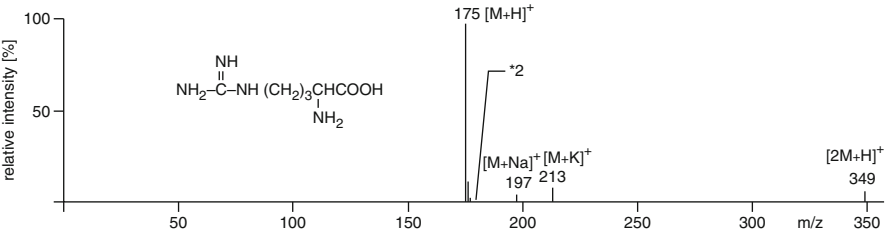

Fig. 8.14 The FD mass spectrum of arginine, $M_r = 174$, desorbed from an untreated metal wire emitter in the presence of alkali ions (Adapted from Ref. [44] by permission. © John Wiley & Sons, 1977)

Two major concepts of ion formation and desorption have been suggested, but it has remained a matter of debate whether the concept of *field-induced desolvation* [94–96] or that of *ion evaporation* [97, 98] more appropriately describes the event. Although different in several aspects, the models are coherent in that ions are created in the condensed phase and subsequently desorbed into the gas phase. Both recognize the electric field as the driving force to effect extraction of ionic species after charge separation within the layer adsorbed onto the emitter surface.

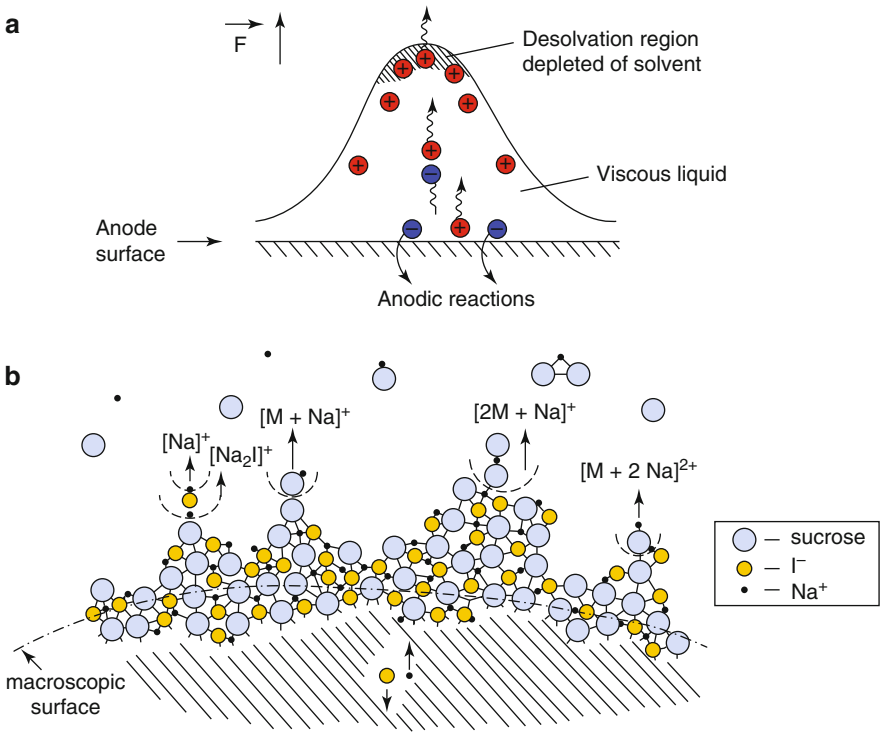

Fig. 8.15 The desolvation of ions. (**a**) Charge separation inside a protuberance, (**b**) continuous reconstruction of the surface allows for successive rupture of intermolecular bonds and stepwise desolvation of the ions (Reproduced from Ref. [96] by permission. © Elsevier Science, 1984)

Protuberances are assumed to develop from where ions can escape into the gas phase as a result of the field-enhancing effect of these protrusions. The differences of the models may in part be attributed to the different experimental and theoretical approaches. The model of the Röllgen group is much based on microscopic observation of protuberances from glassy sample layers (Fig. 8.15) [94, 95], whereas the Derrick group assumes their size to be a thousand-fold smaller (Fig. 8.16) [97]. Thus, the latter emphasizes the role of mobility of molecules instead of microscopic viscous flow of the surface layer.

8.6.3 Cluster Ion Formation in FD-MS

Highly polar analytes which strongly tend towards cationization, frequently form cluster ions such as $[n\text{M+H}]^+$ and $[n\text{M+alkali}]^+$ in addition to $[\text{M+H}]^+$ and $[\text{M+alkali}]^+$ ions. A priori, there is no reason why these cluster ions should not be interpreted as resulting from "impurities". However, the sequence of events can serve as a reliable criterion to distinguish components of higher molecular weight

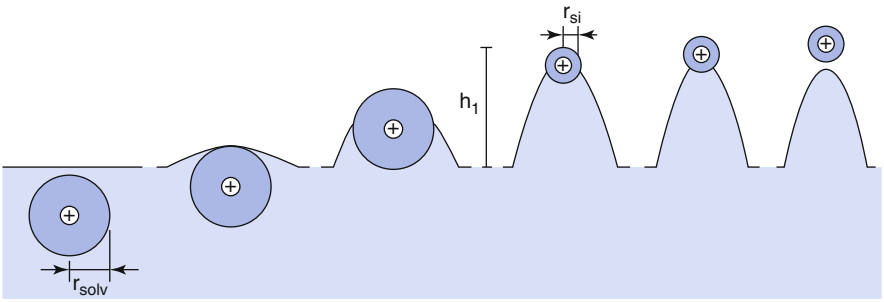

Fig. 8.16 Schematic model for ion evaporation. r_{solv} is the radius of the solvation sphere, r_{si} the radius of the separating ion, and h_1 the height of the protuberance when the radius of its parabolic tip equals r_{si} (Reproduced from Ref. [98] by permission. © Elsevier Science, 1987)

from cluster ions. Cluster ions are preferably formed when the coverage of the emitter surface is still high, i.e., in the beginning of desorption. As desorption proceeds, the probability for cluster ion formation decreases, because the surface layer is diminished. In addition, a continuously rising emitter heating current leads to further thermal decomposition of clusters. Whereas cluster ions decrease in abundance, true higher-mass components require higher emitter temperature to become mobile and ionized thereafter (cf. Sect. 8.4.1). Doubly charged cluster ions, e.g., $[M+2Na]^{2+}$, may also occur. Such doubly or even multiply charged ions can serve to extend the mass range accessible by FD-MS [26].

Cluster ion formation of polar molecules During the acquisition of an FD mass spectrum of a putatively clean disaccharide, a series of ions at higher m/z was observed in addition to $[M+H]^+$, m/z 341 and $[M+Na]^+$, m/z 363. Those ions could be interpreted either in terms of cluster ions or of higher oligosaccharides, respectively. The high-mass ions were only observed soon after the onset of desorption, while their abundance decreased remarkably at somewhat higher emitter current. Thereby, these signals could be assigned to cluster ions such as $[2M+Na]^+$, m/z 703, and $[3M+Na]^+$, m/z 1043 (Fig. 8.17).

Cluster ions or real high-mass component?
Cluster ions of the general formula $[nM+X]^+$, less frequently also $[nM]^{+\bullet}$, mainly appear at the onset of desorption and then decrease in abundance along with the diminishing amount of sample on the emitter. Finally, cluster ions disappear towards the end of desorption. Whether or not the observed peaks at higher m/z correspond to cluster ions can thus be answered by watching the intensity of cluster ion peaks along the period of desorption/ionization.

(continued)

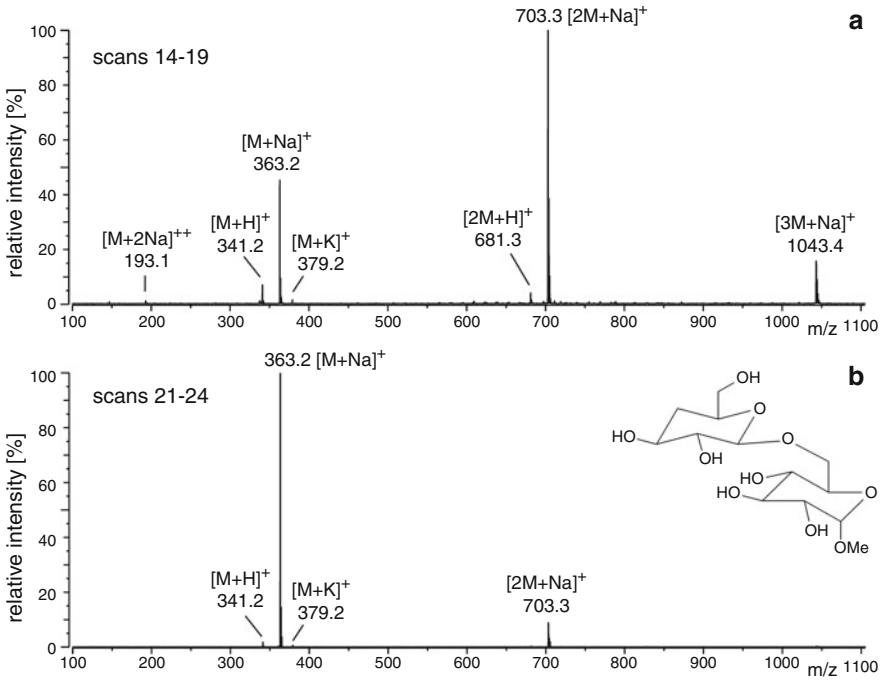

Fig. 8.17 FD mass spectra of a disaccharide (**a**) at the beginning of desorption, (**b**) towards end of desorption [99] (By courtesy of H. Friebolin, Heidelberg University)

Generally, the amount of cluster ion production increases (*i*) at high sample load on the emitter and (*ii*) with higher polarity of the analyte (cf. Sect. 8.6.4).

The value of $\Delta m/z$ between adjacent cluster ion peaks directly reflects the mass of the neutral analyte M. This can also be exploited to identify whether M is detected as $M^{+\bullet}$, $[M+H]^+$, or $[M+Na]^+$.

8.6.4 FD-MS of Ionic Analytes

The intact cation C^+ of an ionic analyte of the general composition $[C^+A^-]$ always causes the base peak in positive-ion FD mass spectra. In addition, singly charged cluster ions of the $[C_nA_{n-1}]^+$ type are observed [100, 101]. Their abundance and the maximum of n varies depending on the ionic species encountered as well as on the actual experimental parameters such as temperature and sample load of the emitter (Figs. 8.18 and 8.19). The advantage of these cluster ions is that the mass difference between the members of the series corresponds to $[C^+A^-]$. Thus, the counterion A^-

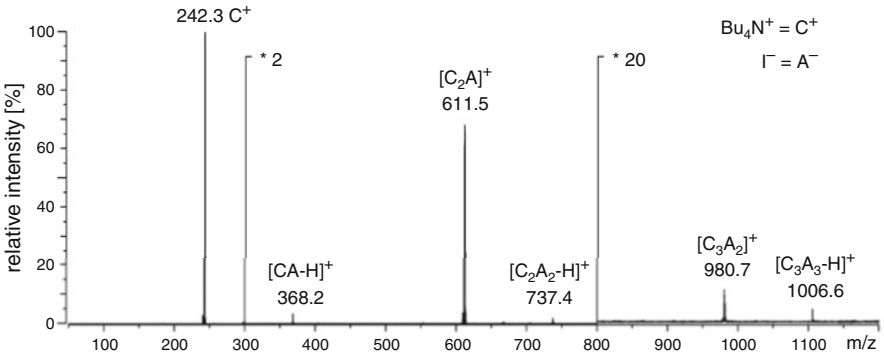

Fig. 8.18 FD mass spectrum of $[(n\text{-}C_4H_9)_4N]^+ I^-$. The intact ammonium ion is detected at m/z 242; additional signals are due to cluster ions. (For the EI spectrum cf. Sect. 6.11.4)

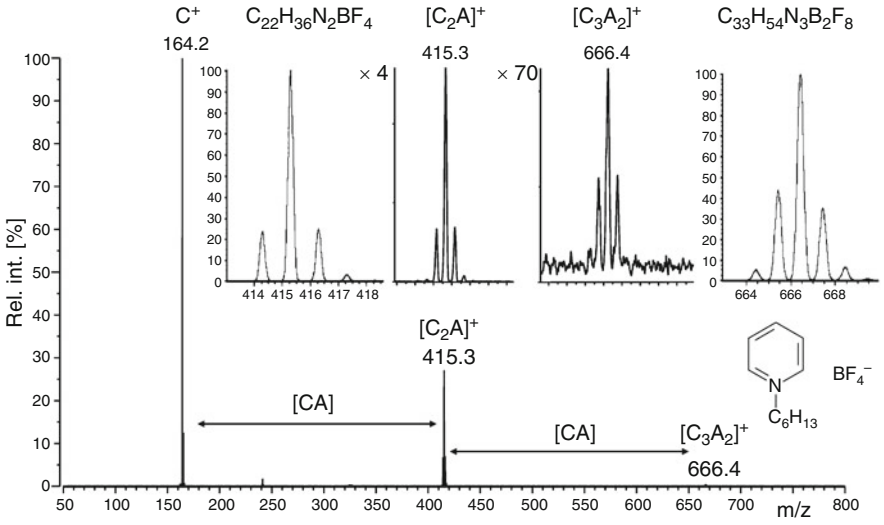

Fig. 8.19 LIFDI mass spectrum of *N*-hexylpyridinium tetrafluoroborate in methanol at a concentration of 0.1 µl ml^{-1} scanned over the m/z 50–800 range. The *insets* show the $[C_2A]^+$ and $[C_3A_2]^+$ cluster ions for comparison of the experimental and calculated isotopic patterns that are characteristic of one and two boron atoms, respectively. The mass of [CA] is obtained from $\Delta(m/z)$ between adjacent cluster ion peaks (Reproduced from Ref. [110] with permission. © Elsevier Science Publishers, 2007)

can be determined by subtraction of the mass of C^+. Moreover, the isotopic pattern of the anion is reflected in the cluster ion signals, facilitating the identification of chloride and bromide, for example. Interestingly, ionic species corresponding to some sort of "molecular ion of the salt" can also be formed. Usually, such ions are of much lower intensity than the even-electron cluster ions. Applications of FD-MS to detect cations are manifold and include organic cations [16, 20, 100–104] as well

as inorganic ones [105, 106] even down to the trace level [107], e.g., for trace-metal analysis in physiological fluids of patients suffering from multiple sclerosis [108].

Zwitterions are generally not easy to analyze by MS. Depending on the acidity of the proton-donating site and on the basicity of the proton-accepting site either the cationic or the anionic species can be formed preferentially. Adding acids to the solution of the analyte prior to loading of the emitter can significantly enhance the signal resulting from the protonated species [109].

Cluster ions reveal cation and anion of salts Ionic liquids (ILs) are perfect representatives of ionic analytes. LIFDI (essentially FD, cf. Sect. 8.6) spectra of ILs such as *N*-hexylpyridinium tetrafluoroborate (Fig. 8.19) are dominated by the cation peak, C^+ here at *m*/*z* 164, that is accompanied by a strong first cluster ion signal, $[(C^+)_2{+}BF_4^-]^+$ at *m*/*z* 415, and by a weak second cluster ion signal. The corresponding boron isotopic patterns (B_1 and B_2) are clearly visible. Furthermore, the softness of the FD process is demonstrated by the fact that even the weakly bound cluster ions exhibit almost no fragmentation in metastable ion spectra, but require collisions to induce dissociation [110].

8.6.5 Temporal Evolution of FD Spectral Acquisition

During an FD run, the FD emitter heating current is generally ramped from 0 to 2 mA to several tens of milliamperes to effect mobilization and desorption/ionization of the analyte on the emitter surface. Thus, a typical total ion chromatogram (TIC) shows a section of very low intensity up to the onset of desorption. There, the TIC rises steeply to the maximum of ion production and then falls quickly after the complete sample has been consumed. The final FD spectrum is best obtained by addition of those scans exhibiting good signal intensity.

FD analysis of an organic solid compound The FD spectrum of α-cyano-4-hydroxycinnamic acid, $C_{10}H_7NO_3$, (CHCA, a matrix compound in MALDI-MS) depicts the typical process of mass spectral acquisition in FD-MS (Fig. 8.20). During the first 35 scans there is almost no desorption, then the analyte is desorbed and ionized during scans 35–46 (EHC ca. 25–30 mA), and finally, the TIC drops after consumption of the sample. To achieve good signal-to-noise ratio, scans 37–44 where accumulated. The resulting FD spectrum mainly shows the $M^{+\bullet}$ ion at *m*/*z* 189.1, which is accompanied by a $[2M]^{+\bullet}$ cluster ion at *m*/*z* 378.1. Both ionic species are also accompanied by fragment ion peaks of very low intensity corresponding to some loss of $OH^\bullet$ and H_2O from $M^{+\bullet}$ and $[2M]^{+\bullet}$ ions, respectively.

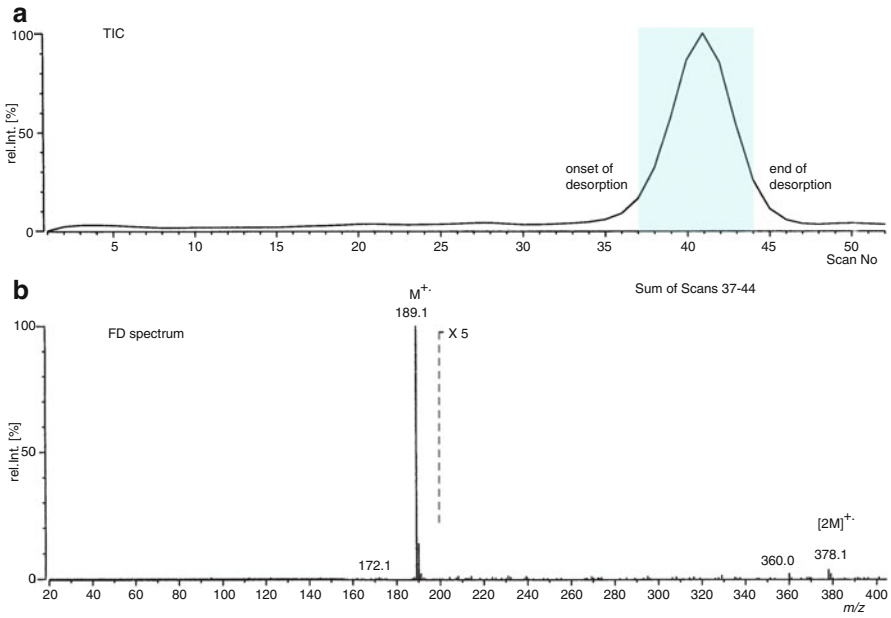

Fig. 8.20 Acquisition of an FD mass spectrum of CHCA. (**a**) TIC, (**b**) resulting FD spectrum. Desorption/ionization occurs during scans No. 35–46. Scans 37–44 where accumulated to provide the final FD spectrum, which mainly shows the $M^{+\bullet}$ ion at *m*/*z* 189.1 and a $[2M]^{+\bullet}$ cluster ion at *m*/*z* 378.1

Shape of the TIC
Pure analytes often show a comparatively sharp onset of desorption. Desorption then lasts for several scans until the sample is consumed. Finally, the intensity of the signals rapidly drops to zero again. In case of mixtures, some fractionation by molecular weight of the components is observed (Fig. 8.21).

8.6.6 Best Anode Temperature and Thermal Decomposition

The onset of desorption of an analyte depends not solely on its intrinsic properties, but also on the extraction voltage and the applied emitter heating current. FD spectra are typically acquired while the *emitter heating current* (EHC) is increased at a constant rate (1–8 mA min^{-1}). Alternatively, the heating can be regulated in a emission-controlled manner [55–57]. The desorption usually begins before the competing thermal decomposition of the analytes becomes severe. Nevertheless, increasing temperature of the emitter transfers additional thermal energy onto the desorbing ions, thereby effecting some fragmentation. The optimum temperature of

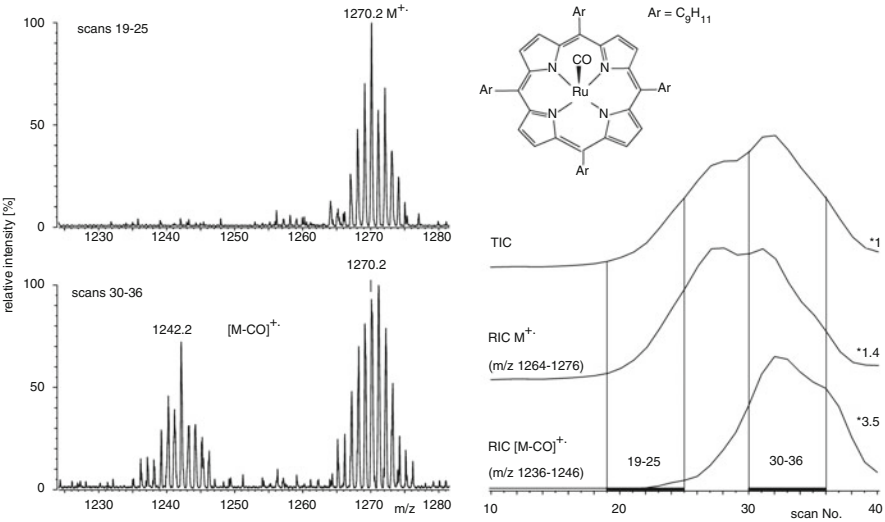

Fig. 8.21 Thermal CO loss during FD measurement of a ruthenium-carbonyl-porphyrin complex (Adapted from Ref. [111] by permission. © IM Publications, 1997)

the emitter where a sufficiently intense signal at the lowest level of fragmentation is obtained has been termed *best anode temperature* (BAT) [19, 37].

FD spectrum of a ruthenium-carbonyl-porphyrin complex The FD spectrum of a ruthenium-carbonyl-porphyrin complex shows an isotopic pattern very close to the theoretical distribution (Sect. 3.2). The loss of the carbonyl ligand chiefly results from thermal decomposition. A spectrum accumulated close to BAT (scans 19–25, EHC 25–30 mA) is nearly devoid of CO loss, while a spectrum accumulated of scans 30–36 (35–40 mA) shows significant CO loss (Fig. 8.21). This is demonstrated by comparison of the total ion chromatogram (TIC) with the reconstructed ion chromatogram (RIC) of $M^{+\bullet}$ and $[M–CO]^{+\bullet}$. The FD spectrum of a lower-mass complex was essentially devoid of signals of CO loss because lower emitter currents were sufficient to effect desorption [111].

8.6.7 FD-MS of Polymers

FD-MS is well suited for the analysis of low- to medium-polarity synthetic oligomers and polymers [26, 27, 70, 74, 75, 77, 112–114]. In advantageous cases, polymer molecules beyond molecular weights of 10,000 u can be measured [115]. Besides the mass analyzer used, limiting factors for the mass range are thermal decomposition of polymer and presence or absence of charge-stabilizing groups. Polystyrene, for example, with its combination of aromatic rings and low polarity is close to an ideal case for FD-MS. Heteroatoms are also useful because of

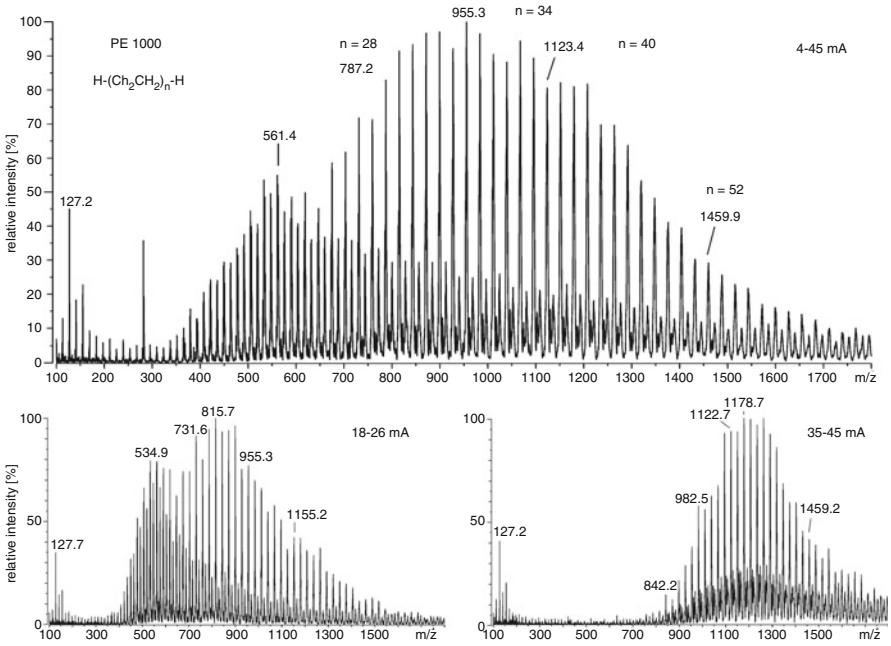

Fig. 8.22 FD spectra of PE 1000 (emitter potential 10 kV, EHC 4–45 mA). *Insets* show selected ranges corresponding to different EHCs (Adapted from Ref. [77] by permission. © IM Publications, 2000)

their general capability to serve as proton- or metal ion-accepting sites. The worst case for MS is that of polyethylene (PE) [74, 75, 77]: the FD mass spectra of PE oligomers can be obtained up to *m*/*z* 3500; however, starting at around C_{40} hydrocarbons, field-induced and thermally induced dehydrogenation can no longer be suppressed and thermal decomposition of the hydrocarbon chains start playing a role above 2000 u.

FD mass spectrum of polyethylene The FD mass spectrum of polyethylene of nominal average molecular weight 1000 u (PE 1000) was obtained by summing of all scans where desorption occurred, i.e., over the 4–45 mA EHC range (Fig. 8.22) [77]. The result represents the molecular weight distribution of the polymer. The according experimental average molecular weight can be calculated by means of Eq. 3.2 (Sect. 3.1). The fractionating effect of emitter heating and the significant changes in spectral appearance are demonstrated by the spectra in the lower part of the figure showing two selected portions of the total ion desorption.

8.6.8 Negative-Ion Field Desorption – An Exotic Exception

Negative-ion FD-MS for the direct detection of the anion A^- and cluster ions of the general composition $[C_{n-1}A_n]^-$ can, in principle, be performed [116, 117]. Nonetheless, negative-ion FD-MS has remained an exception. This is due to the fact that electrons are easily emitted from activated emitters well before negative ions start to desorb. Then, the strong emission of electrons causes a spark discharge that ends up in the destruction of the emitter. Low emitter voltages and larger emitter–counter electrode distance can help to avoid such problems [118]. Neutral analytes can give rise to $[M–H]^-$ ions or products of nucleophilic addition, e.g., $[M+Cl]^-$ ions [119]. Thus, if anions are of interest, they are generally analyzed indirectly by FD-MS via the formation of cluster ions with their positive counterion.

With the advent of fast atom bombardment (FAB, Chap. 10), the interest in negative-ion FD-MS vanished. Nowadays, matrix-assisted laser desorption/ionization (MALDI, Chap. 11), or electrospray ionization (ESI, Chap. 12) are by far preferred for analyzing anions.

8.6.9 Types of Ions in FD-MS

At first sight, FD produces a disadvantageous variety of ions depending on the polarity of the analyte and on the presence or absence of impurities such as alkali metal ions. However, with some knowledge of the ions formed, the signals can be deconvoluted without difficulty (Table 8.2).

Never one adduct alone
One type of alkali adduct ion almost never occurs exclusively, i.e., $[M+H]^+$, $[M+Na]^+$ and $[M+K]^+$ (M+1, M+23 and M+39) are observed with varying relative intensities at 22 u and 16 u distance, respectively. This facilitates the recognition of those peaks and effectively allows for the assignment of the molecular weight.

Table 8.2 Ions formed by FD

Method	Analytes	Ions formed
FD	Nonpolar	$M^{+\bullet}$, M^{2+}, occasionally $M^{3+\bullet}$
FD	Medium polarity	$M^{+\bullet}$, M^{2+} and/or $[M+H]^+$, $[M+alkali]^+$, occasionally $[2M]^{+\bullet}$ and/or $[2M+H]^+$, $[2M+alkali]^+$, rarely $[M+2H]^{2+}$, $[M+2\ alkali]^{2+}$
FD	Polar	$[M+H]^+$, $[M+alkali]^+$, often $[2M+H]^+$, $[2M+alkali]^+$, occasionally $[nM+H]^+$, $[nM+alkali]^+$, rarely $[M+2H]^{2+}$, $[M+2\ alkali]^{2+}$
FD	Ionic[a]	C^+, $[C_n+A_{n-1}]^+$, rarely $[CA]^{+\bullet}$

[a]Comprising cation C^+ and anion A^-

8.7 Liquid Injection Field Desorption Ionization

Numerous analytes could be good candidates for FD-MS, but undergo immediate decomposition by reacting with ambient air and/or water during conventional emitter loading. Emitter loading under inert conditions such as in a glove box does not really avoid the problem, because the emitter still needs to be mounted to the probe before insertion into the vacuum lock.

Liquid injection field desorption ionization (LIFDI) presents a major breakthrough for FD-MS of reactive analytes [29, 120]. The risk of decomposition before starting the measurement is greatly reduced because the analyte, dissolved at about 0.1–0.2 mg ml^{-1}, can be handled under inert conditions. It is transported through a fused silica capillary by the sucking action of the ion source vacuum and then spreads out over the entire emitter driven by capillary forces and adsorption. Careful alignment of the sample transfer capillary with respect to the emitter axis is crucial for reliable wetting. The small volume of solvent transferred (ca. 40 nl) evaporates within seconds. As the sample is supplied from the "backside" to the emitter, there neither is a need to remove the capillary during the measurement, nor to change the adjustment of the emitter inside the ion source (Fig. 8.23). Instead, the emitter interrupts the contact to the capillary as it slightly bends toward the counter electrode as soon as the high voltage is switched on. Thus, LIFDI simplifies the delicate procedure of emitter loading and allows for its repeated loading without breaking the vacuum between successive measurements. This also avoids frequent focusing of the ion source [29, 110, 121]. Together with faster ramping of the EHC, up to 30 mA min^{-1} as enabled by lower sample load, this causes up to tenfold reduced measurement times in LIFDI as compared to conventional FD-MS. In any other respect, FD and LIFDI spectra are equivalent.

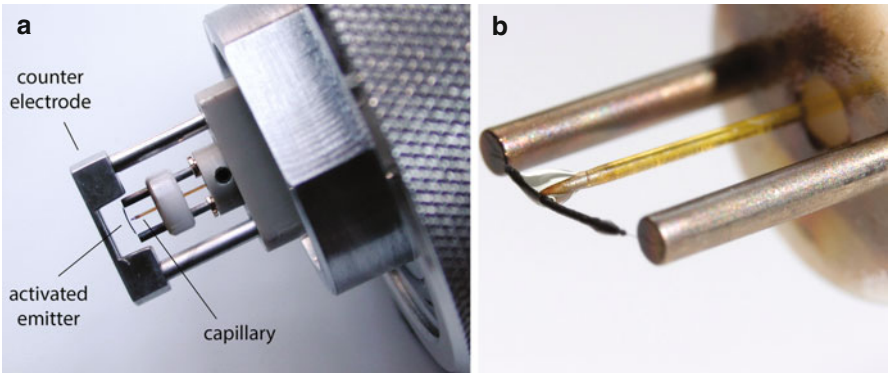

Fig. 8.23 (**a**) LIFDI probe tip with the fused silica capillary that delivers the sample to the "backside" of the activated emitter; here, the counter electrode is part of the probe, and (**b**) wetting of the emitter with solvent spreading out over the activated zone. The 13-μm tungsten wire connecting this section to the posts is barely visible (By courtesy of Linden CMS, Leeste, Germany)

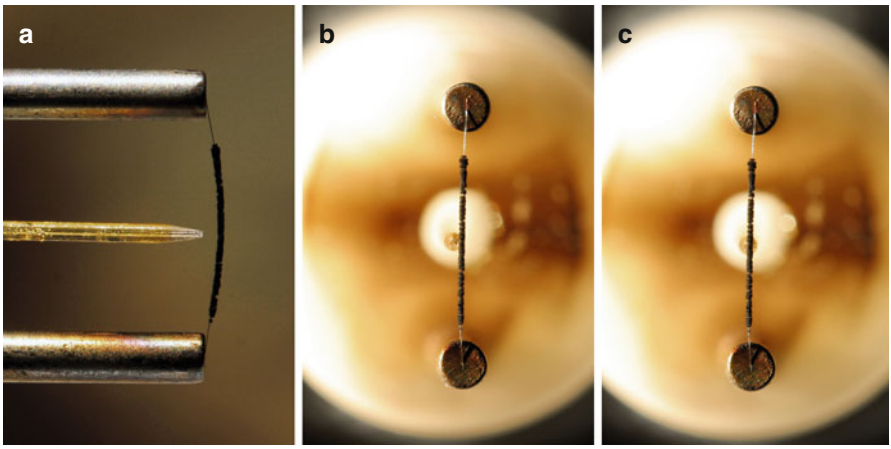

Fig. 8.24 Alignment of the fused silica capillary on the emitter axis; the photographs are similar to what would be observed using a 8× magnifying glass. (**a**) Side view to show the distance between the tip of the capillary and the activated emitter, (**b**, **c**) on axis views. In (**b**) the capillary is left side off-axis while in (**c**) it is well aligned

The majority of LIFDI applications either deals with sensitive compounds such as transition metal complexes [29, 121, 122] or belongs to the group of petroleomics applications [32, 123–125]. Using an extremely low liquid flow rate even allows to continuously deliver sample solution to an emitter at high voltage, permiting continuous-flow (CF-)LIFDI experiments [33, 126]. More recently, an automated LIFDI system has been introduced [127].

8.7.1 Positioning of the Capillary

Accurate positioning of the silica capillary that delivers the analyte solution to the emitter inside the ion source is crucial for LIFDI operation. The tip of the capillary has to approach as closely as possible without ever touching the emitter. Furthermore, it needs to be aligned in order to allow the emerging drop to bridge the gap between the capillary exit and the activated emitter. The simplest way to accomplish this seemingly tricky task is to align the capillary before insertion of the probe. To do so, a magnifying glass (8–10 fold) is recommended. Also, it is important to observe the adjustment on-axis of the capillary, as looking at the assembly in a slightly sideways manner would cause erroneous alignment due to parallax error (Fig. 8.24). The capillary is then positioned by turning a small screw located in the base of the emitter holder.

LIFDI-MS of sensitive compounds Transition metal complexes are readily analyzed by LIFDI-MS. A dichloro nickel carbene complex dissolved in acetonitrile not only forms the expected $[M–Cl]^+$ ion, *m*/*z* 375.3, but also a molecular ion,

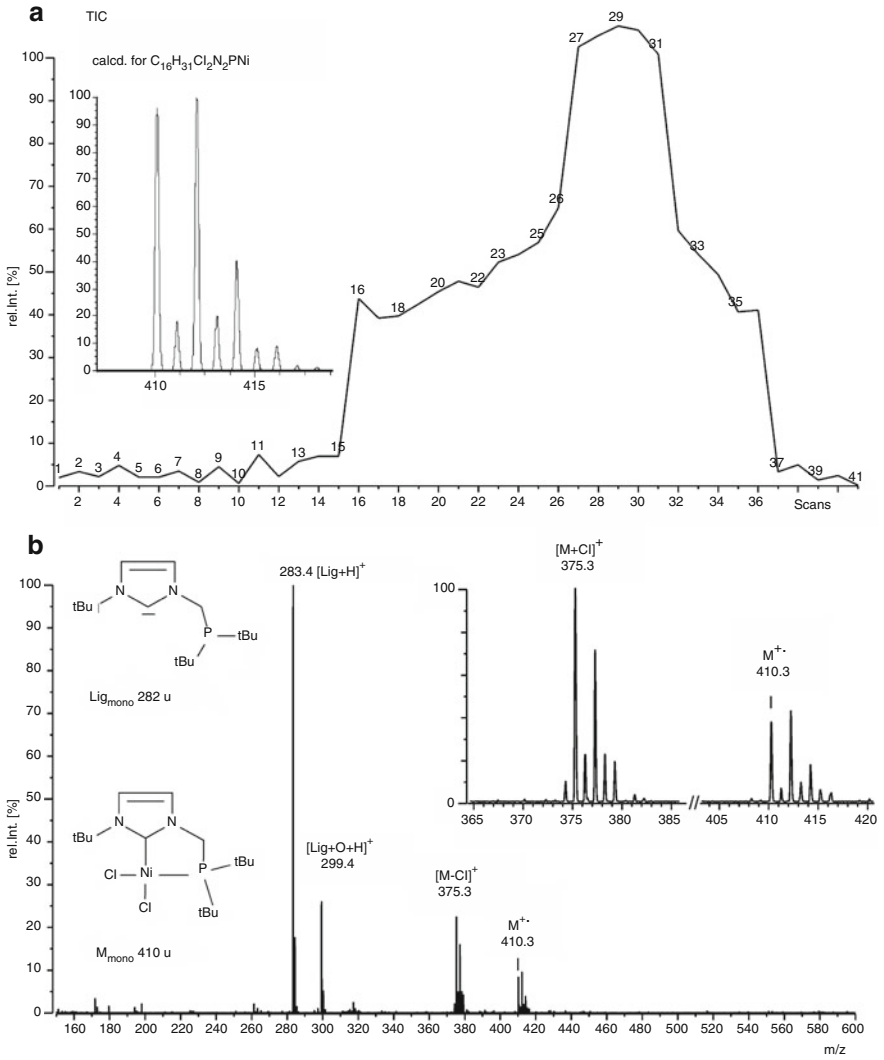

Fig. 8.25 (**a**) TIC and (**b**) LIFDI mass spectrum obtained from a nickel carbene complex in acetonitrile solution shows peaks due to excess free ligand $[Lig+H]^+$, *m*/*z* 283.4, and its oxide $[Lig+O+H]^+$, *m*/*z* 299.4, plus those corresponding to the complex. Note the intense $M^{+\bullet}$ ion at *m*/*z* 410.3 accompanying the $[M–Cl]^+$ ion at *m*/*z* 375.3. The isotopic pattern of the molecular ion is in good agreement with the calculated isotopic distribution (cf. inserts) (Reproduced from Ref. [121] with permission. © Springer-Verlag, Heidelberg, 2006)

m/*z* 410.3, of somewhat lower abundance. The isotopic patterns of the signals are in very good agreement with the calculated isotopic distributions (Fig. 8.25). Peaks due to the free ligand and its oxide are also observed. The corresponding TIC is

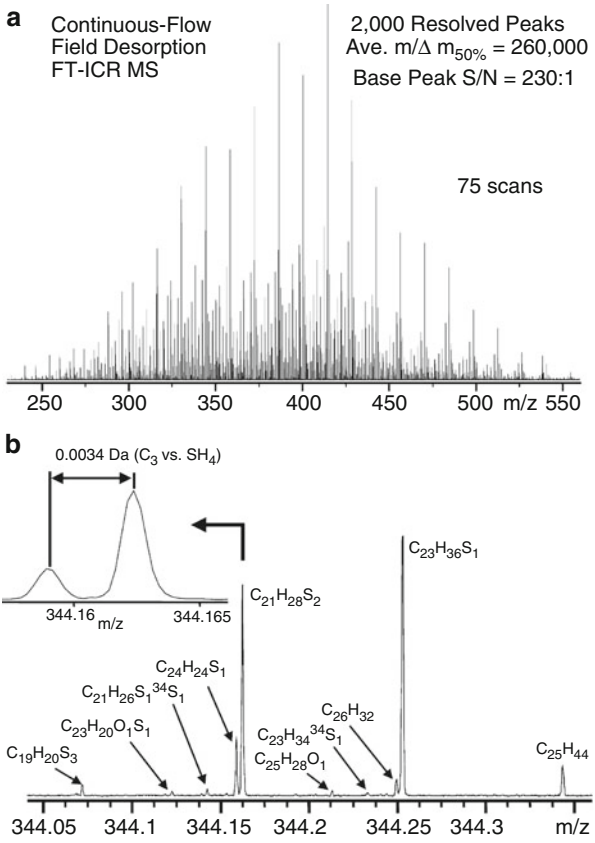

Fig. 8.26 CF-LIFDI-FT-ICR mass spectral analysis of a refinery process stream sample. (**a**) Spectrum as obtained from 75 single spectra accumulated during 1 h. (**b**) Extreme mass scale expansion at nominal *m/z* 344 from the broadband mass spectrum reveals the complexity of the sample. The resolution of the 3.4×10^{-3} u distant C_3 vs. SH_4 doublet can be observed at *m/z* 344.25 and separately in the inset at *m/z* 344.16 (Adapted from Ref. [33] with permission. © John Wiley & Sons Ltd, 2004)

typical for FD experiments and clearly reveals the onset of desorption/ionization at medium EHC and the completion of the measurement when the sample is consumed [121].

Continuous-flow LIFDI-FT-ICR-MS Extremely complex crude oil fractions with each component at a very low concentration can be analyzed by continuous-flow LIFDI-FT-ICR-MS. CF-LIFDI delivers improved spectral quality as a stable FD-generated ion current can be sustained to allow for measurement times totaling up to 1 h. With the ionizing high voltage switched on, the sample solution (0.1 mg ml^{-1}) is delivered at 75 nl min^{-1} through a 10 µm i.d. capillary onto the emitter which is moderately heated using an EHC of 15 mA. The example shows the CF-LIFDI-FT-ICR spectrum of a refinery process stream sample (Fig. 8.26) [33].

8.8 General Properties of FI-MS and FD-MS

8.8.1 Sensitivity of FI-MS and FD-MS

In FD mode, the sensitivity (Sect. 1.6) of magnetic sector instruments is about 4×10^{-11} C μg^{-1} for the $[M+H]^+$ ion of cholesterol, m/z 387, at $R = 1000$. This is 10^4 times less than specified for those instruments in EI mode and 10^3 times less than for CI mode.

In FI mode, the sensitivity of such instruments is about 4×10^{-9} A Pa^{-1} for the molecular ion of acetone, m/z 58, at $R = 1000$. This corresponds to an ion current of 4×10^{-13} A at a realized ion source pressure of 10^{-4} Pa.

Although the ion currents produced by FI/FD ion sources are by orders of magnitude smaller than those from EI or CI ion sources, the detection limits are quite good. In general, about 0.1 ng of sample yield a sufficient signal-to-noise ratio (S/N $\geq$ 10) in FD-MS. This is because most of the ion current is collected in a single ionic species (including the isotopologs). Furthermore, the background of FI/FD ion sources is very clean, providing a good signal-to-background ratio.

Comparison of sensitivity data The comparison of 70-eV EI, CI, NICI and FI on the average reveals a 200-fold lower total ion current from FI as compared to EI. If only molecular ion peak intensities are compared, the FI spectra become much more appealing (Fig. 8.27) [86]. The concentration of the ion current on the molecular ions and the concomitant clarity of FI spectra are certainly the most attractive features of FI-MS.

8.8.2 Analytes and Practical Considerations for FI, FD, and LIFDI

Analytes for FI have to be evaporated prior to ionization, and thus any sample suitable for EI (Sect. 5.10) or CI (Sect. 7.10) yields low-fragmentation FI mass spectra. For FD and LIFDI, the analyte should be soluble to at least 0.01 mg ml^{-1} in some solvent. Concentrations of 0.1–2 mg ml^{-1} are ideal for FD and about 0.1–0.2 mg ml^{-1} should be used for LIFDI. Significantly higher sample loads result in overloading the emitter, and in turn cause its destruction due to electric discharge. In case of extremely low solubility, repeated application of solution to the emitter is also possible. For FD, fine suspensions or dispersions are acceptable, whereas these will block the capillary in LIFDI. Pure water tends not to wet the emitter surface – a problem that can be circumvented by addition of some methanol before transferring the solution to the emitter. Whatever the solvent for FD, it should be volatile enough to evaporate prior to introduction of the probe into the vacuum lock, while small volumes of dimethylformamide or dimethylsulfoxide, for example, can also be evaporated in the rough vacuum of the vacuum lock. The analyte may be neutral or ionic. However, anions are usually detected solely in an indirect manner, i.e., from corresponding cluster ions. Solutions containing metal salts, e.g., from buffers or excess of noncomplexed metals, are to be avoided,

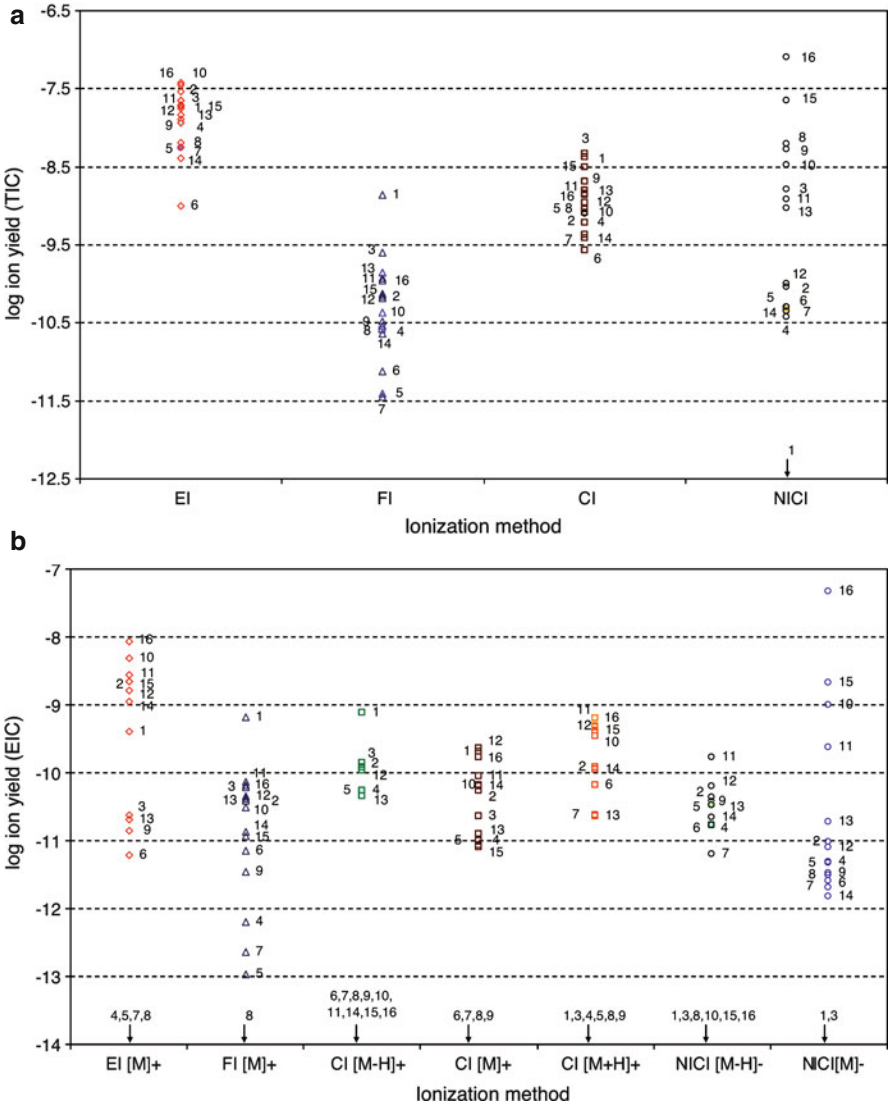

Fig. 8.27 Comparison of (**a**) total ion currents and (**b**) ion currents due to molecular ions or otherwise ionized intact molecules typical for GC-MS as obtained by 70-eV EI, FI, positive-ion CI and negative-ion CI both using methane reagent gas (Reproduced from Ref. [86] with permission. © John Wiley & Sons, Ltd., 2009)

because sudden desorption of the metal ions at higher emitter current often leads to rupture of the emitter. A mass range up to 3000 u is easily covered by FD, and cases reaching up to 10,000 u have been reported.

8.8.3 Mass Analyzers for FI and FD

In FI and FD, ions of 10–12 keV kinetic energy are generated as a continuous ion current. Compared to EI or CI the ion current is weak and tends to fluctuate. The voltage drop across the whiskers (roughly proportional to the whisker length) causes an energy spread of the ions which results in poor resolution with single-focusing magnetic sector instruments [45]. Therefore, double-focusing magnetic sector instruments were the standard in FD-MS for decades. Although linear quadrupoles have been adapted to FI/FD ion sources rather successfully [128, 129], they never became widespread with FI/FD. More recently, oaTOF and FT-ICR analyzers have been equipped with FD/LIFDI sources [34, 35, 123, 126, 127, 130, 131].

Most promising in terms of performance per instrument cost and size is the approach to attach LIFDI to Orbitrap analyzers, in particular to the Thermo Fisher Exactive and Exactive-Q series of instruments. With these particular instruments, the LIFDI source is mounted "at the rear" end, i.e., via the HCD cell (Sect. 9.10). In case of the Exactive-Q type, this unconventional way of mounting the LIFDI source sacrifices the ability to use the instrument's tandem MS capabilities in LIFDI mode, while, on the other hand, it permits to keep the atmospheric pressure source ready while switching back and forth between ESI or APCI and LIFDI operation.

LIFDI of Grubb's catalyst Olefin metathesis by use of Grubbs catalyst, $C_{46}H_{65}Cl_2N_2PRu$ (Grubbs type II), is a common process in preparative organic chemistry. The air- and moisture-sensitive catalyst has been analyzed by using an Exactive Orbitrap instrument with a prototype LIFDI source attached via the HCD cell. The molecular ion signal in this spectrum exhibits about $R = 40.000$. The mass errors of all major peaks are below 1 mu when compared to the calculated isotopic pattern for $[C_{46}H_{65}Cl_2N_2PRu]^{+\bullet}$ (Fig. 8.28).

8.9 FI, FD, and LIFDI at a Glance

Basic Principle

Field ionization (FI) and field desorption (FD) rely on the ionization of neutrals by action of very strong electric fields in the order of 10 V nm^{-1}. The electric field enables the detachment of an electron from the neutral via a tunneling mechanism. While the electron moves into the field anode (aka field emitter) the resulting molecular ion gets ejected from the surface. Field ionization as a mechanism of ion formation can occur in both the gas phase or in the condensed phase at the emitter surface. The technique is also termed *field ionization* when the analyte is supplied via the gas phase to effect ionization of gaseous neutrals. It is termed *field desorption* when the analyte is deposited onto the field emitter prior to exposure to the electric field. Liquid injection field desorption/ionization is a special variant of sample supply for FD-MS. LIFDI allows for sample deposition under inert conditions and enables quicker and smoother operation of FD.

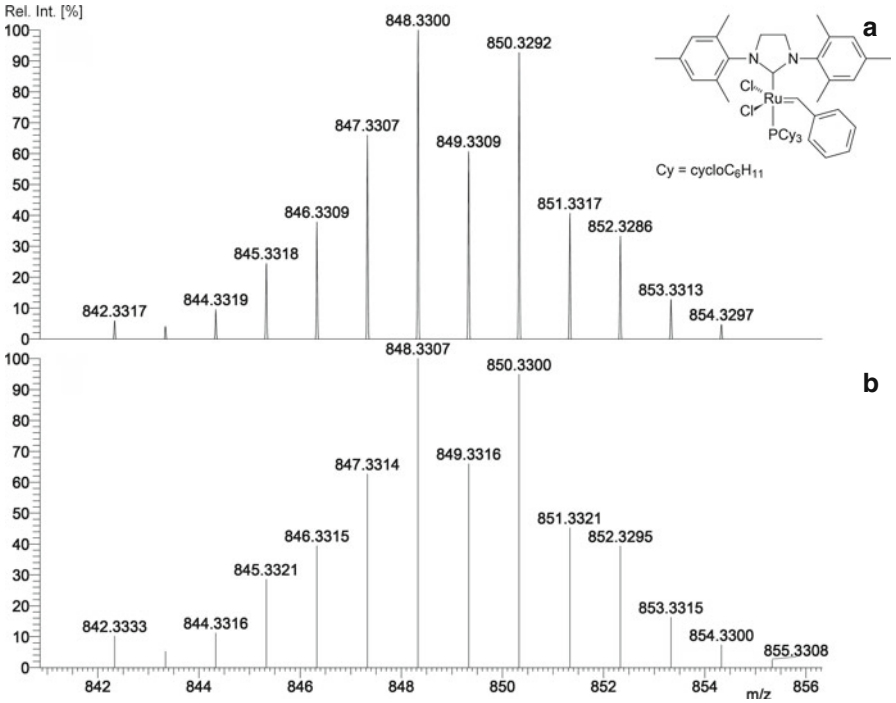

Fig. 8.28 Partial LIFDI spectrum of Grubbs catalyst as obtained by using an Exactive Orbitrap instrument with a prototype source attached via the HCD cell. (**a**) Molecular ion signal, (**b**) calculated isotopic pattern for $[C_{46}H_{65}Cl_2N_2PRu]^{+\bullet}$ (Reproduced with kind permission of Linden CMS, Leeste)

Analytes for FI-MS

Analytes need to be vaporized prior to ionization. Thus, sample supply can be performed from a reservoir inlet, from a sample vial attached to a direct insertion probe, or via a gas chromatograph. The analyte may have low to medium polarity. Normally, FI can be employed for analytes up to about 1000 u.

Analytes for FD-MS

Analytes should preferably be soluble in standard solvents (DMF and DMSO should be avoided due to insufficient volatility). Solutions of 0.1–2.0 mg ml^{-1} are suitable for deposition on the emitter. If necessary, even fine suspensions or emulsions may be transferred onto the emitter. The analyte may have low to high polarity and may also be ionic. FD is suitable to analyze molecules up to 2000–3000 u, depending on their thermal stability.

Analytes for LIFDI-MS

Analytes should preferably be soluble in standard solvents (DMF and DMSO should be avoided due to insufficient volatility). Solutions of 0.1–0.2 mg ml^{-1} are

suitable for transfer through the fused silica capillary. Suspensions or emulsion are to be avoided. The analyte may have low to high polarity and may also be ionic. As LIFDI offers sample deposition under inert conditions, the sample can be highly sensitive to air and/or moisture. The mass range of FD applies analogously.

Polarity
FI exclusively generates positive ions. Apart from some rare exceptions, FD and LIFDI are exclusively operated in positive-ion mode. Anions of salts can be identified due to cluster ion formation.

Softness of Ionization
FI and FD are extremely soft ionization methods as the process of ionization does not impart energy onto the incipient molecular ions. Fragmentation, if any, generally occurs as a result of thermal energy required to effect evaporation or desorption/ionization of larger analyte species. Occasionally, field-induced dissociation or collision-induced dissociation during ion transfer into the mass analyzer may also result in fragmentation or ion losses.

Instrumentation
For decades, magnetic sector instruments have been the classic mass analyzers for FI and FD. Time-of-flight instruments have replaced many of them. Attachment of FD or LIFDI to FT-ICR or Orbitrap analyzers is still an exception but highly attractive in terms of resolving power and mass accuracy.

Accurate Mass
High-resolution and, more importantly, accurate mass data is difficult to obtain if internal mass calibration is required as is the case with magnetic sector instruments. Often, it is just impossible to effect ionization of both analyte and calibration compound simultaneously. The use of single-point corrections (lock mass) on TOF analyzers provides a notable advantage. Best results are to be expected in conjunction with FT-ICR and Orbitrap instruments, which allow to rely on external calibration.

Dissemination and Availability
FI, FD, and LIFDI are generally available as optional ionization techniques of instruments otherwise equipped with vacuum ion sources such as electron ionization (EI) or chemical ionization (CI). Adaptions to other systems can be provided upon request. The use of these techniques is not as widespread as EI, ESI, MALDI, and related ionization methods.

References

1. Müller EW (1953) Feldemission. Ergebn Exakt Naturw 27:290–360. doi:10.1007/BFb0110808
2. Gomer R, Inghram MG (1955) Applications of Field Ionization to Mass Spectrometry. J Am Chem Soc 77:500. doi:10.1021/ja01607a096

3. Inghram MG, Gomer R (1954) Mass-Spectrometric Analysis of Ions from the Field Microscope. J Chem Phys 22:1279–1280. doi:10.1063/1.1740380
4. Inghram MG, Gomer R (1955) Mass-Spectrometric Investigation of the Field Emission of Positive Ions. Z Naturforsch A 10:863–872. doi:10.1515/zna-1955-1113
5. Beckey HD (1959) Mass Spectrographic Investigations, Using a Field Emission Ion Source. Z Naturforsch A 14:712–721. doi:10.1515/zna-1959-0805
6. Beckey HD (1962) Field-Ionization Mass Spectra of Organic Molecules. Normal C_1 to C_9 Paraffins. Z Naturforsch A 17:1103–1111. doi:10.1515/zna-1962-1211
7. Beckey HD, Wagner G (1963) Analytical Use of an Ion Field Mass Spectrometer. Fresenius Z Anal Chem 197:58–80. doi:10.1007/BF00468727
8. Beckey HD (1963) Mass Spectrometric Analysis with a New Source for the Production of Ion Fields at Thin Wires or Metal Edges. Fresenius Z Anal Chem 197:80–90. doi:10.1007/BF00468728
9. Beckey HD, Wagner G (1965) Field Ionization Mass Spectra of Organic Molecules. II. Amines. Z Naturforsch A 20:169–175. doi:10.1515/zna-1965-0201
10. Beckey HD, Schulze P (1965) Field Ionization Mass Spectra of Organic Molecules. III. *N*-Paraffins Up to C_{16} and Branched Paraffins. Z Naturforsch A 20:1329–1335. doi:10.1515/zna-1965-1017
11. Beckey HD (1965) Analysis of Solid Organic Natural Products by Field Ionization Mass Spectrometry. Fresenius Z Anal Chem 207:99–104. doi:10.1007/BF00573238
12. Beckey HD (1966) Comparison of Field Ionization and Chemical Ionization Mass Spectra of Decane Isomers. J Am Chem Soc 88:5333–5335. doi:10.1021/ja00974a061
13. Beckey HD (1969) Field Desorption Mass Spectrometry: A Technique for the Study of Thermally Unstable Substances of Low Volatility. Int J Mass Spectrom Ion Phys 2:500–503. doi:10.1016/0020-7381(69)80047-1
14. Beckey HD, Heindrichs A, Winkler HU (1970) New Field Desorption Techniques. Int J Mass Spectrom Ion Phys 3:A9–A11. doi:10.1016/0020-7381(70)80009-2
15. Beckey HD (1971) Field-Ionization Mass Spectrometry. Pergamon, Elmsford
16. Sammons MC, Bursey MM, White CK (1975) Field Desorption Mass Spectrometry of Onium Salts. Anal Chem 47:1165–1166. doi:10.1021/ac60357a051
17. Beckey HD, Schulten HR (1975) Field Desorption Mass Spectrometry. Angew Chem Int Ed 14:403–415. doi:10.1002/anie.197504031
18. Lehmann WD, Schulten HR (1976) Physikalische Methoden in der Chemie: Massenspektrometrie II CI-, FI- und FD-MS. Chem Unserer Zeit 10:163–174. doi:10.1002/ciuz.19760100602
19. Beckey HD (1977) Principles of Field Desorption and Field Ionization Mass Spectrometry. Pergamon Press, Oxford
20. Larsen E, Egsgaard H, Holmen H (1978) Field Desorption Mass Spectrometry of 1-Methylpyridinium Salts. Org Mass Spectrom 13:417–424. doi:10.1002/oms.1210130710
21. Wood GW (1982) Field Desorption Mass Spectrometry: Applications. Mass Spectrom Rev 1:63–102. doi:10.1002/mas.1280010106
22. Schulten HR (1983) Analytical Applications of Field Desorption Mass Spectrometry. In: Benninghoven A (ed) Ion Formation from Organic Solids. Springer, Heidelberg
23. Lattimer RP, Schulten HR (1989) Field Ionization and Field Desorption Mass Spectrometry: Past, Present, and Future. Anal Chem 61:1201A–1215A. doi:10.1021/ac00196a721
24. Olson KL, Rinehart KL (1993) Field Desorption, Field Ionization, and Chemical Ionization Mass Spectrometry. Methods Carbohyd Chem 9:143–164
25. Del Rio JC, Philp RP (1999) Field Ionization Mass Spectrometric Study of High Molecular Weight Hydrocarbons in a Crude Oil and a Solid Bitumen. Org Geochem 30:279–286. doi:10.1016/S0146-6380(99)00014-5
26. Guo X, Fokkens RH, Peeters HJW, Nibbering NMM, de Koster CG (1999) Multiple Cationization of Polyethylene Glycols in Field Desorption Mass Spectrometry: A New Approach to Extend the Mass Scale on Sector Mass Spectrometers. Rapid Commun Mass

Spectrom 13:2223–2226. doi:10.1002/(SICI)1097-0231(19991115)13:21<2223::AID-RCM756>3.0.CO;2-C
27. Lattimer RP (2001) Field ionization (FI-MS) and field desorption (FD-MS). In: Montaudo G, Lattimer RP (eds) Mass Spectrometry of Polymers. CRC Press, Boca Raton
28. Linden HB (2002) Quick Soft Analysis of Sensitive Samples Under Inert Conditions by In-Source Liquid Injection FD. Proc 50th Ann Conf Mass Spectrom Allied Topics, MPL 373. 2002. Orlando, ASMS
29. Linden HB (2004) Liquid Injection Field Desorption Ionization: A New Tool for Soft Ionization of Samples Including Air-Sensitive Catalysts and Non-Polar Hydrocarbons. Eur J Mass Spectrom 10:459–468. doi:10.1255/ejms.655
30. Hsu CS, Green M (2001) Fragment-Free Accurate Mass Measurement of Complex Mixture Components by Gas Chromatography/Field Ionization-Orthogonal Acceleration Time-of-Flight Mass Spectrometry: An Unprecedented Capability for Mixture Analysis. Rapid Commun Mass Spectrom 15:236–239. doi:10.1002/1097-0231(20010215)15:3<236::AID-RCM197>3.0.CO;2-B
31. Qian K, Dechert GJ (2002) Recent Advances in Petroleum Characterization by GC Field Ionization Time-of-Flight High-Resolution Mass Spectrometry. Anal Chem 74:3977–3983. doi:10.1021/ac020166d
32. Schaub TM, Hendrickson CL, Qian K, Quinn JP, Marshall AG (2003) High-Resolution Field Desorption/Ionization Fourier Transform Ion Cyclotron Resonance Mass Analysis of Non-polar Molecules. Anal Chem 75:2172–2176. doi:10.1021/ac020627v
33. Schaub TM, Linden HB, Hendrickson CL, Marshall AG (2004) Continuous-Flow Sample Introduction for Field Desorption/Ionization Mass Spectrometry. Rapid Commun Mass Spectrom 18:1641–1644. doi:10.1002/rcm.1523
34. Linden HB, Gross JH (2011) A Liquid Injection Field Desorption/Ionization-Electrospray Ionization Combination Source for a Fourier Transform Ion Cyclotron Resonance Mass Spectrometer. J Am Soc Mass Spectrom 22:2137–2144. doi:10.1007/s13361-011-0259-9
35. Linden HB, Gross JH (2012) Reduced Fragmentation in Liquid Injection Field Desorption/Ionization-Fourier Transform Ion Cyclotron Resonance Mass Spectrometry by Use of Helium for the Thermalization of Molecular Ions. Rapid Commun Mass Spectrom 26:336–344. doi:10.1002/rcm.5335
36. Gomer R (1994) Field Emission, Field Ionization, and Field Desorption. Surf Sci 299 (300):129–152. doi:10.1016/0039-6028(94)90651-3
37. Prókai L (1990) Field Desorption Mass Spectrometry. Marcel Dekker, New York
38. Todd JFJ (1995) Recommendations for Nomenclature and Symbolism for Mass Spectroscopy Including an Appendix of Terms Used in Vacuum Technology. Int J Mass Spectrom Ion Proc 142:211–240. doi:10.1016/0168-1176(95)93811-F
39. Ligon WV Jr (1979) Molecular Analysis by Mass Spectrometry. Science 205:151–159. doi:10.1126/science.205.4402.151
40. Miyamoto K, Fujimaki S, Ueda Y (2009) Development of a New Electron Ionization/Field Ionization Ion Source for Gas Chromatography/Time-of-Flight Mass Spectrometry. Rapid Commun Mass Spectrom 23:3350–3354. doi:10.1002/rcm.4256
41. Schröder E (1991) Massenspektrometrie – Begriffe und Definitionen. Springer, Heidelberg
42. Derrick PJ, Robertson AJB (1973) Field Ionization Mass Spectrometry with Conditioned Razor Blades. Int J Mass Spectrom Ion Phys 10:315–321. doi:10.1016/0020-7381(73)83009-8
43. Giessmann U, Heinen HJ, Röllgen FW (1979) Field Desorption of Nonelectrolytes Using Simply Activated Wire Emitters. Org Mass Spectrom 14:177–179. doi:10.1002/oms.1210140314
44. Heinen HJ, Giessmann U, Röllgen FW (1977) Field Desorption of Electrolytic Solutions Using Untreated Wire Emitters. Org Mass Spectrom 12:710–715. doi:10.1002/oms.1210121112

45. Beckey HD, Krone H, Röllgen FW (1968) Comparison of Tips, Thin Wires, and Sharp Metal Edges as Emitters for Field Ionization Mass Spectrometry. J Sci Instrum 1:118–120. doi:10.1088/0022-3735/1/2/308
46. Beckey HD, Hilt E, Schulten HR (1973) High Temperature Activation of Emitters for Field Ionization and Field Desorption Spectrometry. J Phys E:Sci Instrum 6:1043–1044. doi:10.1088/0022-3735/6/10/028
47. Linden HB, Hilt E, Beckey HD (1978) High-Rate Growth of Dendrites on Thin Wire Anodes for Field Desorption Mass Spectrometry. J Phys E:Sci Instrum 11:1033–1036. doi:10.1088/0022-3735/11/10/019
48. Rabrenovic M, Ast T, Kramer V (1981) Alternative Organic Substances for Generation of Carbon Emitters for Field Desorption Mass Spectrometry. Int J Mass Spectrom Ion Phys 37:297–307. doi:10.1016/0020-7381(81)80051-4
49. Linden HB, Beckey HD, Okuyama F (1980) On the Mechanism of Cathodic Growth of Tungsten Needles by Decomposition of Hexacarbonyltungsten Under High-Field Conditions. Appl Phys 22:83–87. doi:10.1007/BF00897937
50. Bursey MM, Rechsteiner CE, Sammons MC, Hinton DM, Colpitts T, Tvaronas KM (1976) Electrochemically Deposited Cobalt Emitters for Field Ionization and Field Desorption Mass Spectrometry. J Phys E Sci Instrum 9:145–147. doi:10.1088/0022-3735/9/2/026
51. Matsuo T, Matsuda H, Katakuse I (1979) Silicon Emitter for Field Desorption Mass Spectrometry. Anal Chem 51:69–72. doi:10.1021/ac50037a025
52. Okuyama F, Shen GH (1981) Ion Formation Mechanisms in Field-Desorption Mass Spectrometry of Semirefractory Metal Elements. Int J Mass Spectrom Ion Phys 39:327–337. doi:10.1016/0020-7381(81)87006-4
53. Kümmler D, Schulten HR (1975) Correlation Between Emitter Heating Current and Emitter Temperature in Field Desorption Mass Spectrometry. Org Mass Spectrom 10:813–816. doi:10.1002/oms.1210100918
54. Winkler HU, Linden B (1976) On the Determination of Desorption Temperatures in Field Desorption Mass Spectrometry. Org Mass Spectrom 11:327–329. doi:10.1002/oms.1210110314
55. Schulten HR, Lehmann WD (1977) High-Resolution Field Desorption Mass Spectrometry. Part VII. Explosives and Explosive Mixtures. Anal Chim Acta 93:19–31. doi:10.1016/0003-2670(77)80003-2
56. Schulten HR, Nibbering NMM (1977) An Emission-Controlled Field Desorption and Electron Impact Spectrometry Study of Some *N*-Substituted Propane and Butane Sultams. Biomed Mass Spectrom 4:55–61. doi:10.1002/bms.1200040108
57. Schulten HR (1978) Recent Advances in Field Desorption Mass Spectrometry. Adv Mass Spectrom 7A:83–97
58. Beckey HD (1964) Molecule Dissociation by High Electric Fields. Z Naturforsch A 19:71–83. doi:10.1515/zna-1964-0114
59. Severin D (1976) Molecular Ion Mass Spectrometry for the Analysis of High- and Nonboiling Hydrocarbon Mixtures. Erdöl und Kohle Erdgas Petrochemie Vereinigt mit Brennstoff-Chemie 29:13–18
60. Mead L (1968) Field Ionization Mass Spectrometry of Heavy Petroleum Fractions. Waxes. Anal Chem 40:743–747. doi:10.1021/ac60260a040
61. Scheppele SE, Hsu CS, Marriott TD, Benson PA, Detwiler KN, Perreira NB (1978) Field-Ionization Relative Sensitivities for the Analysis of Saturated Hydrocarbons from Fossil-Energy-Related Materials. Int J Mass Spectrom Ion Phys 28:335–346. doi:10.1016/0020-7381(78)80077-1
62. Gross JH (2008) Molecular Ions of Ionic Liquids in the Gas Phase. J Am Soc Mass Spectrom 19:1347–1352. doi:10.1016/j.jasms.2008.06.002
63. Röllgen FW, Beckey HD (1970) Surface Reactions Induced by Field Ionization of Organic Molecules. Surf Sci 23:69–87. doi:10.1016/0039-6028(70)90006-3

64. Schulten HR, Beckey HD (1974) Criteria for Distinguishing Between $M^{+\cdot}$ and $[M+H]^+$ Ions in Field Desorption Mass Spectra. Org Mass Spectrom 9:1154–1155. doi:10.1002/oms.1210091111
65. Goldenfeld IV, Korostyshevsky IZ, Nazarenko VA (1973) Multiple Field Ionization. Int J Mass Spectrom Ion Phys 11:9–16. doi:10.1016/0020-7381(73)80050-6
66. Helal AI, Zahran NF (1988) Field Ionization of Indene on Tungsten. Int J Mass Spectrom Ion Proc 85:187–193. doi:10.1016/0168-1176(88)83014-3
67. Röllgen FW, Heinen HJ (1975) Formation of Multiply Charged Ions in a Field Ionization Mass Spectrometer. Int J Mass Spectrom Ion Phys 17:92–95. doi:10.1016/0020-7381(75)80010-6
68. Röllgen FW, Heinen HJ (1975) Energetics of Formation of Doubly Charged Benzene Ions by Field Ionization. Z Naturforsch A 30:918–920. doi:10.1515/zna-1975-6-735
69. Röllgen FW, Heinen HJ, Levsen K (1976) Doubly-Charged Fragment Ions in the Field Ionization Mass Spectra of Alkylbenzenes. Org Mass Spectrom 11:780–782. doi:10.1002/oms.1210110712
70. Neumann GM, Cullis PG, Derrick PJ (1980) Mass Spectrometry of Polymers: Polypropylene Glycol. Z Naturforsch A 35:1090–1097. doi:10.1515/zna-1980-1015
71. McCrae CE, Derrick PJ (1983) The Role of the Field in Field Desorption Fragmentation of Polyethylene Glycol. Org Mass Spectrom 18:321–323. doi:10.1002/oms.1210180802
72. Heine CE, Geddes MM (1994) Field-Dependent $[M-2H]^{+\cdot}$ Formation in the Field Desorption Mass Spectrometric Analysis of Hydrocarbon Samples. Org Mass Spectrom 29:277–284. doi:10.1002/oms.1210290603
73. Klesper G, Röllgen FW (1996) Field-Induced Ion Chemistry Leading to the Formation of $[M-2_nH]^{+\cdot}$ and $[2M-2_mH]^{+\cdot}$ Ions in Field Desorption Mass Spectrometry of Saturated Hydrocarbons. J Mass Spectrom 31:383–388. doi:10.1002/(SICI)1096-9888(199604)31:4<383::AID-JMS311>3.0.CO;2-1
74. Evans WJ, DeCoster DM, Greaves J (1995) Field Desorption Mass Spectrometry Studies of the Samarium-Catalyzed Polymerization of Ethylene Under Hydrogen. Macromolecules 28:7929–7936. doi:10.1021/ma00127a046
75. Evans WJ, DeCoster DM, Greaves J (1996) Evaluation of Field Desorption Mass Spectrometry for the Analysis of Polyethylene. J Am Soc Mass Spectrom 7:1070–1074. doi:10.1016/1044-0305(96)00043-8
76. Gross JH, Vékey K, Dallos A (2001) Field Desorption Mass Spectrometry of Large Multiply Branched Saturated Hydrocarbons. J Mass Spectrom 36:522–528. doi:10.1002/jms.151
77. Gross JH, Weidner SM (2000) Influence of Electric Field Strength and Emitter Temperature on Dehydrogenation and C-C Cleavage in Field Desorption Mass Spectrometry of Polyethylene Oligomers. Eur J Mass Spectrom 6:11–17. doi:10.1255/ejms.300
78. Chait EM, Shannon TW, Perry WO, Van Lear GE, McLafferty FW (1969) High-Resolution Field-Ionization Mass Spectrometry. Int J Mass Spectrom Ion Phys 2:141–155. doi:10.1016/0020-7381(69)80014-8
79. Forehand JB, Kuhn WF (1970) High Resolution Field Ionization Mass Spectrometry of the Condensable Phase of Cigaret Smoke. Anal Chem 42:1839–1841. doi:10.1021/ac50160a073
80. Schulten HR, Beckey HD, Meuzelaar HLC, Boerboom AJH (1973) High-Resolution Field Ionization Mass Spectrometry of Bacterial Pyrolysis Products. Anal Chem 45:191–195. doi:10.1021/ac60323a039
81. Schulten HR, Marzec A, Simmleit N, Dyla P, Mueller R (1989) Thermal Behavior and Degradation Products of Differently Ranked Coals Studied by Thermogravimetry and High-Resolution Field-Ionization Mass Spectrometry. Energy Fuel 3:481–487. doi:10.1021/ef00016a010
82. Games DE, Jackson AH, Millington DS (1973) Applications of Field Ionization Mass Spectrometry in the Analysis of Organic Mixtures. Tetrahedron Lett 14:3063–3066. doi:10.1016/S0040-4039(01)96320-8

83. Damico JN, Barron RP (1971) Application of Field Ionization to Gas-Liquid Chromatography-Mass Spectrometry (GLC-MS) Studies. Anal Chem 43:17–21. doi:10.1021/ac60296a032
84. Briker Y, Ring Z, Iacchelli A, McLean N, Rahimi PM, Fairbridge C, Malhotra R, Coggiola MA, Young SE (2001) Diesel Fuel Analysis by GC-FIMS: Aromatics, *n*-Paraffins, and Isoparaffins. Energy Fuel 15:23–37. doi:10.1021/ef000106f
85. Qian K, Dechert GJ, Edwards KE (2007) Deducing Molecular Compositions of Petroleum Products Using GC-Field Ionization High Resolution Time of Flight Mass Spectrometry. Int J Mass Spectrom 265:230–236. doi:10.1016/j.ijms.2007.02.012
86. Hejazi L, Ebrahimi D, Hibbert DB, Guilhaus M (2009) Compatibility of Electron Ionization and Soft Ionization Methods in Gas Chromatography/Orthogonal Time-of-Flight Mass Spectrometry. Rapid Commun Mass Spectrom 23:2181–2189. doi:10.1002/rcm.4131
87. Kane-Maguire LAP, Kanitz R, Sheil MM (1995) Comparison of Electrospray Mass Spectrometry with Other Soft Ionization Techniques for the Characterization of Cationic Π-Hydrocarbon Organometallic Complexes. J Organomet Chem 486:243–248. doi:10.1016/0022-328X(94)05041-9
88. Rogers DE, Derrick PJ (1984) Mechanisms of Ion Formation in Field Desorption of Oligosaccharides. Org Mass Spectrom 19:490–495. doi:10.1002/oms.1210191006
89. Derrick PJ, Nguyen T-T, Rogers DEC (1985) Concerning the Mechanism of Ion Formation in Field Desorption. Org Mass Spectrom 11:690. doi:10.1002/oms.1210201108
90. Veith HJ, Röllgen FW (1985) On the Ionization of Oligosaccharides. Org Mass Spectrom 11:689–690. doi:10.1002/oms.1210201108
91. Schulten HR, Beckey HD (1972) Field Desorption Mass Spectrometry with High-Temperature Activated Emitters. Org Mass Spectrom 6:885–895. doi:10.1002/oms.1210060808
92. Davis SC, Neumann GM, Derrick PJ (1987) Field Desorption Mass Spectrometry with Suppression of the High Field. Anal Chem 59:1360–1362. doi:10.1021/ac00136a021
93. Veith HJ (1977) Alkali Ion Addition in FD Mass Spectrometry. Cationization and Protonation-Ionization Methods in the Application of Nonactivated Emitters. Tetrahedron 33:2825–2828. doi:10.1016/0040-4020(77)80275-5
94. Giessmann U, Röllgen FW (1981) Electrodynamic Effects in Field Desorption Mass Spectrometry. Int J Mass Spectrom Ion Phys 38:267–279. doi:10.1016/0020-7381(81)80072-1
95. Röllgen FW (1983) Principles of field desorption mass spectrometry. In: Benninghoven A (ed) Ion Formation from Organic Solids. Springer, Heidelberg
96. Wong SS, Giessmann U, Karas M, Röllgen FW (1984) Field Desorption of Sucrose Studied by Combined Optical Microscopy and Mass Spectrometry. Int J Mass Spectrom Ion Proc 56:139–150. doi:10.1016/0168-1176(84)85038-7
97. Derrick PJ (1986) Mass Spectroscopy at High Mass. Fresenius Z Anal Chem 324:486–491. doi:10.1007/BF00474121
98. Davis SC, Natoli V, Neumann GM, Derrick PJ (1987) A Model of Ion Evaporation Tested Through Field Desorption Experiments on Glucose Mixed with Alkali Metal Salts. Int J Mass Spectrom Ion Proc 78:17–35. doi:10.1016/0168-1176(87)87039-8
99. Reichert H (1997) Monodesoxygenierte Glucosid-Synthese und Kinetikstudien der enzymatischen Spaltung. PhD Thesis. Organisch-Chemisches Institut, Heidelberg University
100. Veith HJ (1976) Field Desorption Mass Spectrometry of Quaternary Ammonium Salts: Cluster Ion Formation. Org Mass Spectrom 11:629–633. doi:10.1002/oms.1210110609
101. Veith HJ (1983) Mass Spectrometry of Ammonium and Iminium Salts. Mass Spectrom Rev 2:419–446. doi:10.1002/mas.1280020402
102. Veith HJ (1980) Collision-Induced Fragmentations of Field-Desorbed Cations. 4. Collision-Induced Fragmentations of Alkylideneammonium Ions. Angew Chem Int Ed 19:541–542. doi:10.1002/anie.198005411

103. Fischer M, Veith HJ (1981) Collision-Induced Fragmentations of Field-Desorbed Cations. 5. Reactions of 2- and 3-Phenyl Substituted Alkylalkylidene Iminium Ions in the Gas Phase. Helv Chim Acta 64:1083–1091. doi:10.1002/hlca.19810640413
104. Miermans CJH, Fokkens RH, Nibbering NMM (1997) A Study of the Applicability of Various Ionization Methods and Tandem Mass Spectrometry in the Analyses of Triphenyltin Compounds. Anal Chim Acta 340:5–20. doi:10.1016/S0003-2670(96)00541-7
105. Röllgen FW, Giessmann U, Heinen HJ (1976) Ion Formation in Field Desorption of Salts. Z Naturforsch A 31:1729–1730. doi:10.1515/zna-1976-1245
106. Röllgen FW, Ott KH (1980) On the Formation of Cluster Ions and Molecular Ions in Field Desorption of Salts. Int J Mass Spectrom Ion Phys 32:363–367. doi:10.1016/0020-7381(80)80019-2
107. Lehmann WD, Schulten HR (1977) Determination of Alkali Elements by Field Desorption Mass Spectrometry. Anal Chem 49:1744–1746. doi:10.1021/ac50020a028
108. Schulten HR, Bohl B, Bahr U, Mueller R, Palavinskas R (1981) Qualitative and Quantitative Trace-Metal Analysis in Physiological Fluids of Multiple Sclerosis Patients by Field Desorption Mass Spectrometer. Int J Mass Spectrom Ion Phys 38:281–295. doi:10.1016/0020-7381(81)80073-3
109. Keough T, DeStefano AJ (1981) Acid-Enhanced Field Desorption Mass Spectrometry of Zwitterions. Anal Chem 53:25–29. doi:10.1021/ac00224a009
110. Gross JH (2007) Liquid Injection Field Desorption/Ionization Mass Spectrometry of Ionic Liquids. J Am Soc Mass Spectrom 18:2254–2262. doi:10.1016/j.jasms.2007.09.019
111. Frauenkron M, Berkessel A, Gross JH (1997) Analysis of Ruthenium Carbonyl-Porphyrin Complexes: A Comparison of Matrix-Assisted Laser Desorption/Ionization Time-of-Flight, Fast-Atom Bombardment and Field Desorption Mass Spectrometry. Eur Mass Spectrom 3:427–438. doi:10.1255/ejms.177
112. Lattimer RP, Harmon DJ, Welch KR (1979) Characterization of Low Molecular Weight Polymers by Liquid Chromatography and Field Desorption Mass Spectroscopy. Anal Chem 51:293–296. doi:10.1021/ac50044a040
113. Craig AC, Cullis PG, Derrick PJ (1981) Field Desorption of Polymers: Polybutadiene. Int J Mass Spectrom Ion Phys 38:297–304. doi:10.1016/0020-7381(81)80074-5
114. Lattimer RP, Schulten HR (1983) Field Desorption of Hydrocarbon Polymers. Int J Mass Spectrom Ion Phys 52:105–116. doi:10.1016/0020-7381(83)85094-3
115. Matsuo T, Matsuda H, Katakuse I (1979) Use of Field Desorption Mass Spectra of Polystyrene and Polypropylene Glycol as Mass References Up to Mass 10000. Anal Chem 51:1329–1331. doi:10.1021/ac50044a050
116. Ott KH, Röllgen FW, Zwinselmann JJ, Fokkens RH, Nibbering NMM (1980) Negative Ion Field Desorption Mass Spectra of Some Inorganic and Organic Compounds. Org Mass Spectrom 15:419–422. doi:10.1002/oms.1210150805
117. Daehling P, Röllgen FW, Zwinselmann JJ, Fokkens RH, Nibbering NMM (1982) Negative Ion Field Desorption Mass Spectrometry of Anionic Surfactants. Fresenius Z Anal Chem 312:335–337. doi:10.1007/BF00470387
118. Mes GF, Van der Greef J, Nibbering NMM, Ott KH, Röllgen FW (1980) The Formation of Negative Ions by Field Ionization. Int J Mass Spectrom Ion Phys 34:295–301. doi:10.1016/0020-7381(80)85043-1
119. Dähling P, Ott KH, Röllgen FW, Zwinselmann JJ, Fokkens RH, Nibbering NMM (1983) Ionization by Proton Abstraction in Negative Ion Field Desorption Mass Spectrometry. Int J Mass Spectrom Ion Phys 46:301–304. doi:10.1016/0020-7381(83)80112-0
120. Linden HB (2001) Electric field-induced ionization of analytes in mass spectrometer by desorption from microdendrite substrates, German Patent No. DE 99-19963317
121. Gross JH, Nieth N, Linden HB, Blumbach U, Richter FJ, Tauchert ME, Tompers R, Hofmann P (2006) Liquid Injection Field Desorption/Ionization of Reactive Transition Metal Complexes. Anal Bioanal Chem 386:52–58. doi:10.1007/s00216-006-0524-0

122. Monillas WH, Yap GPH, Theopold KH (2007) A Tale of Two Isomers: A Stable Phenyl Hydride and a High-Spin ($S = 3$) Benzene Complex of Chromium. Angew Chem Int Ed 46:6692–6694. doi:10.1002/anie.200701933
123. Schaub TM, Hendrickson CL, Quinn JP, Rodgers RP, Marshall AG (2005) Instrumentation and Method for Ultrahigh Resolution Field Desorption Ionization Fourier Transform Ion Cyclotron Resonance Mass Spectrometry of Nonpolar Species. Anal Chem 77:1317–1324. doi:10.1021/ac048766v
124. Fu J, Klein GC, Smith DF, Kim S, Rodgers RP, Hendrickson CL, Marshall AG (2006) Comprehensive Compositional Analysis of Hydrotreated and Untreated Nitrogen-Concentrated Fractions from Syncrude Oil by Electron Ionization, Field Desorption Ionization, and Electrospray Ionization Ultrahigh-Resolution FT-ICR Mass Spectrometry. Energy Fuel 20:1235–1241. doi:10.1021/ef060012r
125. Stanford LA, Rodgers RP, Marshall AG, Czarnecki J, Wu XA (2007) Compositional Characterization of Bitumen/Water Emulsion Films by Negative- and Positive-Ion Electrospray Ionization and Field Desorption/Ionization Fourier Transform Ion Cyclotron Resonance Mass Spectrometry. Energy Fuel 21:963–972. doi:10.1021/ef060291i
126. Schaub TM, Rodgers RP, Marshall AG, Qian K, Green LA, Olmstead WN (2005) Speciation of Aromatic Compounds in Petroleum Refinery Streams by Continuous Flow Field Desorption Ionization FT-ICR Mass Spectrometry. Energy Fuel 19:1566–1573. doi:10.1021/ef049734d
127. Smith DF, Schaub TM, Rodgers RP, Hendrickson CL, Marshall AG (2008) Automated Liquid Injection Field Desorption/Ionization for Fourier Transform Ion Cyclotron Resonance Mass Spectrometry. Anal Chem 80:7379–7382. doi:10.1021/ac801085r
128. Heinen HJ, Hötzel C, Beckey HD (1974) Combination of a Field Desorption Ion Source with a Quadrupole Mass Analyzer. Int J Mass Spectrom Ion Phys 13:55–62. doi:10.1016/0020-7381(74)83005-6
129. Gierlich HH, Heinen HJ, Beckey HD (1975) The Application of Quadrupole Mass Filters in Field Desorption Mass Spectrometry. Biomed Mass Spectrom 2:31–35. doi:10.1002/bms.1200020107
130. Smith DF, Rahimi P, Teclemariam A, Rodgers RP, Marshall AG (2008) Characterization of Athabasca Bitumen Heavy Vacuum Gas Oil Distillation Cuts by Negative/Positive Electrospray Ionization and Automated Liquid Injection Field Desorption Ionization Fourier Transform Ion Cyclotron Resonance Mass Spectrometry. Energy Fuel 22:3118–3125. doi:10.1021/ef8000357
131. Miyabayashi K, Naito Y, Miyake M (2009) Characterization of Heavy Oil by FT-ICR MS Coupled with Various Ionization Techniques. J Jpn Pet Inst 52:159–171. doi:10.1627/jpi.52.159